(2)

AD _____

CONTRACT NO: DAMD17-90-C-0041

TITLE: NEUROPATHOLOGICAL CONSEQUENCES OF EXPOSURE TO SUBLETHAL DOSES OF CYANIDE

PRINCIPAL INVESTIGATOR: Thomas L. Pazdernik, Ph.D.
AUTHORS: Stanley R. Nelson, M.D.
Fred E. Samson, Ph.D.

CONTRACT ORGANIZATION: University of Kansas Medical Center
39th and Rainbow Boulevard
Kansas City, Kansas 66160-7336

REPORT DATE: November 1, 1992

TYPE OF REPORT: Final

PREPARED FOR: U.S. ARMY MEDICAL RESEARCH AND DEVELOPMENT COMMAND
Fort Detrick, Frederick, Maryland 21702-5012

DISTRIBUTION STATEMENT:

Approved for public release; distribution unlimited.

The findings in this report are not to be construed as an official Department of the Army position unless so designated by other authorized documents.

SECURITY CLASSIFICATION OF THIS PAGE

REPORT DOCUMENTATION PAGE

Form Approved OMB No. 0704-0188

1a. REPORT SECURITY CLASSIFICATION Unclassified	1b. RESTRICTIVE MARKINGS
2a. SECURITY CLASSIFICATION AUTHORITY	3. DISTRIBUTION / AVAILABILITY OF REPORT Approved for public release; distribution unlimited
2b. DECLASSIFICATION / DOWNGRADING SCHEDULE	
4. PERFORMING ORGANIZATION REPORT NUMBER(S)	5. MONITORING ORGANIZATION REPORT NUMBER(S)
6a. NAME OF PERFORMING ORGANIZATION University of Kansas Medical Center, School of Medicine 6b. OFFICE SYMBOL (If applicable)	7a. NAME OF MONITORING ORGANIZATION
6c. ADDRESS (City, State, and ZIP Code) Kansas City, KS 66160	7b. ADDRESS (City, State, and ZIP Code)
8a. NAME OF FUNDING / SPONSORING ORGANIZATION U.S. Army Medical Research and Development Command 8b. OFFICE SYMBOL (If applicable)	9. PROCUREMENT INSTRUMENT IDENTIFICATION NUMBER Contract No. DAMD17-90-C-0041
8c. ADDRESS (City, State, and ZIP Code) Fort Detrick Frederick, MD 21702-5012	10. SOURCE OF FUNDING NUMBERS PROGRAM ELEMENT NO. 62787A PROJECT NO. 3M1- 62787A875 TASK NO. AA WORK UNIT ACCESSION NO. DA331031

11. TITLE (Include Security Classification)
Neuropathological consequences of exposure to sublethal doses of cyanide

12. PERSONAL AUTHOR(S)
Pazdernik, Thomas L.; Nelson, Stanley R.; Samson, Fred E.

13a. TYPE OF REPORT	13b. TIME COVERED	14. DATE OF REPORT (Year, Month, Day)	15. PAGE COUNT
Final	FROM 90/1/29 TO 92/7/31	1992 November 1	62

16. SUPPLEMENTARY NOTATION

17. COSATI CODES			18. SUBJECT TERMS (Continue on reverse if necessary and identify by block number)
FIELD	GROUP	SUB-GROUP	Cyanide, local cerebral glucose use, brain edema, intracerebral microdialysis, lactate, ascorbate, potassium, hydrogen peroxide, monoamines, amino acids, RAV
06	15		
06	11		

19. ABSTRACT (Continue on reverse if necessary and identify by block number)

Experiments focused on the effects of cyanide on brain energy metabolism, microdialysis studies (to measure acid products of anaerobic metabolism, brain monoamines and metabolites, redox-active substances and amino acids), edema and histology. Wistar rats were infused iv with sodium cyanide (NaCN) until the animal lost its righting reflex; when righting returned, NaCN infusion was started again. The local cerebral glucose use (LCGU) was measured by the [^{14}C]-2-deoxyglucose (2-DG) procedure. A shift from aerobic to anaerobic metabolism and the oxidation-reduction state of the brain extracellular fluid (ECF) were determined by intracerebral microdialysis. Immediately after iv infusion of NaCN, there is a robust **increase** in glucose use. Also, there is a dramatic increase, up to 5-fold, in lactate in the ECF indicating an increase in anaerobic metabolism. However, at 60 minutes after NaCN, LCGU is **markedly reduced** in all 45 brain regions measured, except for choroid plexus. Thus, the expected increase in glucose use as a result of anaerobic metabolism is brief. The marked increase in acid metabolites of dopamine and serotonin suggest that dopamine and serotonin may participate in the reduction

20. DISTRIBUTION / AVAILABILITY OF ABSTRACT ☐ UNCLASSIFIED/UNLIMITED ☐ SAME AS RPT. ☐ DTIC USERS	21. ABSTRACT SECURITY CLASSIFICATION Unclassified
22a. NAME OF RESPONSIBLE INDIVIDUAL Virginia M. Miller	22b. TELEPHONE (Include Area Code) 301-619-7325 22c. OFFICE SYMBOL SGRD-RMI

DD Form 1473, JUN 86 *Previous editions are obsolete.* SECURITY CLASSIFICATION OF THIS PAGE

FOREWORD

Opinions, interpretations, conclusions and recommendations are those of the author and not necessarily endorsed by the U.S. Army.

_____ Where copyrighted material is quoted, permission has been obtained to use such material.

_____ Where material from documents designated for limited distribution is quoted, permission has been obtained to use the material.

TLP Citations of commercial organizations and trade names in this report do not constitute an official Department of Army endorsement or approval of the products or services of these organizations.

TLP In conducting research using animals, the investigator(s) adhered to the "Guide for the Care and Use of Laboratory Animals," prepared by the Committee on Care and Use of Laboratory Animals of the Institute of Laboratory Resources, National Research Council (NIH Publication No. 86-23, Revised 1985).

_____ For the protection of human subjects, the investigator(s) adhered to policies of applicable Federal Law 45 CFR 46.

_____ In conducting research utilizing recombinant DNA technology, the investigator(s) adhered to current guidelines promulgated by the National Institutes of Health.

PI - Signature _____ DATE Apr. 27, 1993

TABLE OF CONTENTS

Table of Contents

Table of Contents

INTRODUCTION

Cyanide is a rapidly acting metabolic poison, that among other things, interferes with the oxidative generation of free energy in cells. Although the exact chemical details are still unknown, the undissociated form (HCN) appears to block electron transfer in the cytochrome a-a_3 complex (Schubert and Brill, 1968; Isom and Way, 1984; Piantados *et al.*, 1983). Acute cyanide intoxication produces incoordination of movements, convulsions, tremors, changes in EEG, coma, cardiac arrhythmias, and respiratory arrest (Burrows *et al.*, 1982; Persson *et al.*, 1985; Brierley *et al.*, 1976, 1977), all of which are signs indicating central nervous system (CNS) as an early target of HCN toxicity. The brain is particularly vulnerable to cyanide because of its limited anaerobic metabolic capacity and high energy dependence (Johnson *et al.*, 1986; Way, 1984). In fact, lethality from cyanide poisoning results from failure of vital functions of the CNS (Borowitz *et al.*, 1992). Cyanide produces a histotoxic energy failure that is associated with cellular swelling, elevated brain calcium levels, and increased lipid peroxidation (Johnson *et al.*, 1986; 1987; Borowitz *et al.*, 1992). CNS areas that appear to be vulnerable to cyanide-induced damage include: layer IV cortex, hippocampus CA_1, caudate-putamen, globus pallidus, corpus callosum, optic chiasm, and substantia nigra (Hicks, 1950; Levine, 1967; Hirano *et al.*, 1967; Funata *et al.*, 1984; Bass, 1968). Thus, survivors of cyanide intoxication would be prone to have extensive neuronal damage and consequent motor and/or behavior deficits.

The problem under investigation in this contract was the neurochemical mechanism(s) that underlie the neuropathological consequences of sublethal doses of cyanide. The experimental model was adult male laboratory rats exposed to sodium cyanide (NaCN) by controlled iv infusion. The approach was measuring changes in brain regional metabolism with the 2-deoxyglucose (2-DG) procedure and monitoring changes in chemical composition of the

extracellular compartment with the intracerebral microdialysis procedure, and to relate these to behavioral neurotoxicological changes that occur. Although there are reports on changes in tissue chemical composition after cyanide exposure, this proposal is unique in that the extracellular microenvironment of cells is the subject of study. Also, the 2-DG method was used to provide rates of glucose use throughout the brain.

BODY

Experimental Methods:

Animals: Adult male Wistar rats weighing 250-300 g were obtained from SASCO Co. (Omaha, NE). Food and water were provided *ad libitum* and a 12-hour light/dark cycle was maintained. Experiments were conducted in accordance with the guidelines of the National Research Council DHEW Publication No. (NIH) 80-23 (1980).

Agent: NaCN was obtained from Fisher Scientific Co. (Fairlawn, NJ). Cyanide was used in accordance with the security assurances required. All unused NaCN cyanide solutions and contaminated material were alkalinized with 0.1 N NaOH to prevent the escape of hydrogen cyanide (Robinson *et al.*, 1984).

NaCN exposure: Rats were given saline or NaCN by controlled iv infusion (20 µl/min; 4.5-5.0 mg/ml) into the femoral vein. The infusion was temporarily halted when the rat lost its righting reflex and was resumed when righting recurred.

Brain regional metabolism mapping: The method for regional brain glucose utilization was based on that of Sokoloff *et al.* (1977). [^{14}C]-2-DG (specific activity = 55 mCi/mmol; American Radiolabeled Chemicals Inc., St. Louis, MO) was injected iv (100-150 µCi/kg) as a pulse in 0.9% saline. During the first minute immediately following the pulse, 6 timed serial arterial blood samples (50-70 µl) were collected in heparinized hematocrit tubes. Blood samples were then taken every 5 minutes for plasma glucose determinations and [^{14}C] scintillation counting. At the end of the experiment, the rat was decapitated and the brain quickly removed, frozen in freon 12 at -70°C and bagged in plastic airtight bags for storage at -70°C.

Five microliters of each plasma sample were pipetted into 4 ml of scintillation cocktail (Research Products International Corp., Econo-Safe) and counted in a Hewlett-Packard Tri-Carb

Scintillation Counter. Ten microliters of plasma were used to determine plasma glucose levels with a Yellow Springs Instrument Model 23A glucose analyzer (Yellow Springs, OH).

Coronal sections (20 μm) of brain were cut at -20°C and immediately dried on a 55-60°C slide warmer. Adjacent sections were used for autoradiograms and hematoxylin and eosin (H&E) stains. These sections, along with [^{14}C]methyl methacrylate standards, were exposed to Kodak Min-R X-ray film for 21 days. The optical density of a given brain structure was determined by video-computer assisted analysis. For each subject, the average of several optical density readings per brain area, the plasma glucose level and plasma [^{14}C] concentration were used to calculate local cerebral glucose utilization (LCGU) according to the equation developed by Sokoloff *et al.* (1977). The equation and constants used are given in Figure 1.

Microdialysis probe assembly: Two microdialysis probe designs, loop and concentric tubes, were prepared from Dow 50 cellulose membranes (MW cut-off = 5000; O.D. = 250 μm) obtained from a kidney dialysis cartridge. The loop fiber was inserted and glued with epoxy into two 2 cm sections of 23 gauge stainless steel tubing, leaving 6 mm of exposed dialysis fiber length. The concentric tube design microdialysis apparatus consisted of fused silica hollow tubing (Polymicro Technology; I.D. = 75 μm; O.D. = 155 μm) placed inside teflon tubing (30 gauge; 10 mm length) and extended beyond the lumen of the teflon approximately 4 mm. Teflon tubing was added to the rear of the assembly in a "Y" shaped design, the fluid inlet consisting of fused silica inside 24 gauge teflon tubing and the fluid outlet consisting of 30 gauge teflon tubing. The assembled "Y" intersection was secured with contact adhesive and placed in an Eppendorf sample tube cut to 5 mm length and pierced at the bottom with a 21 gauge needle. Casting resin (Castin' Craft clear with surface curing agent and liquid hardener catalyst) was poured into the Eppendorf tubing containing the inlet/outlet intersection. The assembly was allowed to harden and dry overnight. After placing the microdialysis membrane over the

protruding fused silica tubing and inside the 30 gauge teflon tubing, the assembly was secured with contact adhesive, exposing approximately 3 mm of microdialysis membrane as dialysis surface area. In the study where NaCN was delivered via the microdialysis fiber, an I-shaped dialysis probe (BPP-I-8-02, 2 mm dialysis membrane, 220 μm diameter, 50,000 molecular weight cut off, Eicom, Kyoto, Japan) was used.

Perfusion apparatus: A Hamilton Microliter 1000 Series Gas-tight syringe (total volume = 5 cc) with a teflon-tipped plunder was used with a Harvard syringe infusion pump for constant flow delivery. A needle hub was constructed from a teflon dowel rod (O.D. = 13 mm) to accommodate a standard syringe fitting (4 mm width) reduced over a 15 mm length to accommodate 20 gauge teflon tubing (O.D. = 1.0 mm; I.D. = 0.86 mm). The 20 gauge teflon tubing fit snugly over the probe inlet 24 gauge teflon tubing. The seal was further improved at the junction by adding silastic tubing (Dow Corning; O.D. = 1.5 mm; I.D. = 1.0 mm) outside of the teflon tubing.

Fiber implantation: Animals were anesthetized with pentobarbital (40 mg/kg, i.p.) and placed in a stereotaxic apparatus. Anesthesia was maintained with methoxyflurane. A hole was drilled in the appropriate place in the exposed skull to allow placement of the dialysis fiber. The stereotaxic coordinates from Paxinos and Watson (1982) relative to bregma were for right piriform cortex A: - 1.8, L: - 5.7, V: - 9.0 mm. For studies where NaCN was delivered via microdialysis, a guide cannula (G-4, Eicom; Kyoto, Japan) was stereotaxically implanted into the right striatum (A:0.5, L:2.5, V:-4.0 mm from the bregma) followed by insertion of the I-shaped dialysis probe. The experiments were started 24 hours after the fiber implantation. After the experiment was completed, fiber placement was verified histologically.

$$\text{Rate of Reaction} = \frac{\text{Labeled Product Formed in Interval of Time, O to T}}{\left[\text{Isotope Effect Correction Factor}\right]\left[\text{Integrated Specific Activity of Precursor}\right]}$$

Operational Equation of [^{14}C]-2-Deoxyglucose Method:

$$R_i = \frac{\overbrace{C_i^*(T)}^{\text{Total }^{14}\text{C in Tissue at Time, T}} - \overbrace{k_1^* e^{-(k_2^*+k_3^*)T}\int_0^T C_p^* e^{(k_2^*+k_3^*)t}\,dt}^{^{14}\text{C in Precursor Remaining in Tissue at Time, T}}}{\underbrace{\left[\frac{\lambda \cdot V_m^* \cdot K_m}{\phi \cdot V_m \cdot K_m^*}\right]}_{\text{Isotope Effect Correction Factor}}\underbrace{\left[\int_0^T \left(\frac{C_p^*}{C_p}\right)dt}_{\text{Integrated Plasma Specific Activity}} - \underbrace{e^{-(k_2^*+k_3^*)T}\int_0^T \left(\frac{C_p^*}{C_p}\right)e^{(k_2^*+k_3^*)t}\,dt}_{\text{Correction for Lag in Tissue Equilibration with Plasma}}\right]}}$$

Integrated Precursor Specific Activity in Tissue

where

R_i = glucose consumption per gm of tissue

$C_i^*(T)$ = total concentration of [^{14}C]DG and [^{14}C]DG-6-P (determined by quantitative autoradiography) in the tissues at time, T

C_p^* = arterial plasma [^{14}C]DG concentration

C_p = arterial plasma glucose concentration

k_1^* = rate constant for transport of [^{14}C]DG from plasma to tissue precursor pool

k_2^* = rate constant for transport of [^{14}C]DG from tissue back to plasma

k_3^* = rate constant for phosphorylation of [^{14}C]DG

λ = ratio of distribution volume of [^{14}C]DG to that of glucose in the tissue

ϕ = fraction of glucose that, once phosphorylated, is glycolytically and oxidatively metabolized

K_m^* = Michaelis-Menten kinetic constant of hexokinase for [^{14}C]DG

V_{max}^* = maximum velocity of hexokinase for [^{14}C]DG

K_m = Michaelis-Menten constant of hexokinase for glucose

V_{max} = maximum velocity of hexokinase for glucose

$$\frac{[\lambda \cdot Vm^* \cdot Km]}{[\phi \cdot Vm \cdot Km^*]} = 0.481 \pm 0.119$$

Values for constants in Albino Rat (mean values):

Gray matter: $K_1^* = 0.189 \pm 0.012$ (min^{-1})
$K_2^* = 0.245 \pm 0.04$ (min^{-1})
$K_3^* = 0.052 \pm 0.01$ (min^{-1})

White matter: $K_1^* = 0.079 \pm 0.01$ (min^{-1})
$K_2^* = 0.133 \pm 0.05$ (min^{-1})
$K_3^* = 0.02 \pm 0.02$ (min^{-1})

Figure 1. Operational equation of the [^{14}C]-2-deoxyglucose ([^{14}C]-2-DG) method. From Sokoloff, 1976; 1981.

Microdialysis perfusion: All experiments were initiated 1 day after fiber implantation and were done in unanesthetized freely moving rats. The dialysis fiber input was connected to an infusion pump with Teflon tubing and a tubing fluid swivel. The fiber was perfused with Krebs Ringer Bicarbonate (KRB, in mmol/L: NaCl, 122; KCl, 3; $MgSO_4$, 1.2; KH_2PO_4, 0.4; $NaHCO_3$, 25 and $CaCl_2$, 1.2) or Ringer's solution (in mmol/L: NaCl, 148; KCL 3; $CaCl_2$, 2.5) at a flow rate of 2 µl/min with exceptions. Initially, the fiber was perfused with media alone for 2 hours and the samples discarded. The next 4 or 5 samples were used to determine basal levels of the substances to be analyzed. Samples were collected at intervals stated in figures (3-20; 22-24).

Lactate and pyruvate: Twenty microliters of perfusate were used to determine perfusate lactate and pyruvate concentrations by an HPLC method with UV detection at 214 nm. An Alltech Spherisorb (C-8, 5 µm, 250 x 4.6 mm) column was used. The mobile phase consisted of 0.1 M sodium phosphate buffer (adjusted to pH 2.4) at a flow rate of 1.2 ml/min.

[^{14}C]-2-DG in perfusate: In these rats a microdialysis fiber was implanted in the piriform cortex prior to initiation of the 2-DG procedure. The [^{14}C]-2-DG radiolabel was measured in the perfusate samples.

Hydroperoxides: Chemiluminescence: In an MGM Optocomp I luminometer, isoluminol/microperoxidase cocktail in sodium borate buffer was added to 20 µl aliquots of H_2O_2 standards or microdialysis samples treated with perfusion medium or medium containing catalase (50 U/ml). Subsequent chemiluminescence was quantified in relative light units (RLU) using a kinetic analysis protocol of 60 contiguous 4-second counting intervals integrated over time after automatic injection of 300 µl of cocktail into the sample compartment (Yamamoto and Ames, 1987).

Ascorbate and urate analyses: HPLC/ECD Assay: Direct analysis of microdialysates for ascorbate and urate concentrations was done with HPLC electrochemical detection. The mobile phase consisted of sodium acetate (40 mM), dodecyltrimethylammonium chloride (1.5 mM), disodium ethylenediaminetetraacetic acid (0.54 mM) and methanol (7.5%), adjusted to pH 4.6 with glacial acetic acid. Flow rate was 0.8 ml/min. A reverse-phase 5 μm C-18 column, 250 x 4.6 mm, with a C-18 guard column was used for analyte separation with a ESA Coulochem II dual cell detector, the column was kept at 35°C. Cell 2 potential was set a 350 mV with no potential on cell 1. An inline guard cell potential was set at 500 mV.

Monoamines and metabolites: Dopamine, 3,4-dihydroxyphenyl acetic acid (DOPAC), homovanillic acid (HVA), serotonin and 5-hydroxyindole acetic acid (5-HIAA) were quantitated by HPLC with electrochemical detection as described by Westerink *et al.* (1988). The mobile phase consisted of 0.025 M NaH_2 PO_4, 0.15 M citric acid, 300 mg/L 1-octanesulfonic acid, sodium salt, 33.6 mg/L Na_2 EDTA and 22% methanol. Flow rate was 0.8 ml/min. A reverse phase 5 μm C-18 column, 250 x 4.6 mm, with a C-18 guard column was used for analyte separation with a ESA Coulchem II dual cell detector. The column was kept at 35°C. Cell 1 potential was 50 mV, cell 2 potential was 450 mV and the inline guard cell potential was set at 500 mV.

Amino acid analysis: Perfusate samples were analyzed for free amino acids by HPLC using a modification of the procedure described by Lindroth and Mopper (1979) with fluorescence detection (see Wade *et al.*, 1987). In brief, perfusate (10 μl) was reacted with *o*-phthaldialdehyde reagent (20 μl) consisting of 250 μl of *o*-phthaldialdehyde in ethanol (27 mg/ml), 100 μl of phosphate-buffered mercaptoethanol (0.5 mol/L; Sigma), and 9.65 ml of sodium tetraborate (38 mg/L). Following a 2-minute reaction time, 20 μl of the derivatized sample mixture was injected into a HPLC system. Amino acid derivatives were then separated

on a C-18 column (pore size = 5-μm; Adsorbosphere; Alltech Associates, Deerfield, IL, U.S.A.) using an isocratic mobile phase of 65% sodium phosphate buffer (0.1 mol/L, pH 5.5) and 35% methanol.

Brain tissue specific gravity: Regional changes in brain density were measured gravimetrically by modification of the method of Nelson *et al.* (1971). Rats were sacrificed by decapitation, the brains removed (within 2 minutes) and submerged in kerosene (4°C) for dissection. Small tissue samples (about 2 mm^3) were taken bilaterally from the frontal cortex, parietal cortex, piriform cortex, hippocampus, caudate, corpus callosum and dorsal thalamus. Samples were placed in a linear kerosene-bromobenzene gradient column and their position in the column was recorded after 2 minutes. The linearity of the column was determined with glass standards (Nelson and Olson, 1987). The increase in tissue volume, which represents edema fluid, was then calculated from change in specific gravity according to the formula:

$$\text{Percent change in tissue volume as water} = \left[\frac{\text{Control Sp.Gr.} - 1}{\text{Experimental Sp.Gr.} - 1} - 1\right] \text{X } 100$$

Histology: The animals were anesthetized with 40 mg/kg in pentobarbital and perfused by intracardiac injection with 10% buffered formalin. Frozen cryostat sections (20 μm) were used to verify placement of fibers. H&E stained paraffin cut sections (5 μm) were used to identify neuropathology.

Statistics: LCGU data were analyzed with a one-way analysis of variance (ANOVA) followed by a Dunnett's t-test. Significance was set at $p < 0.05$. Data from microdialysis studies were analyzed by repeated analysis of variance. Specific gravity data were analyzed with a Student's t-test.

Results and Discussion:

Brain metabolism studies: To determine the brain regions affected by sublethal doses of cyanide, male rats were given saline or NaCN by controlled iv infusion (20 μl/min; 4.5-5.0 mg/ml) into the femoral vein. The infusion was temporarily halted when the rat lost its righting reflex and infusion resumed when righting recurred. The infusion process lasted 1 hour or until the end of the 45 minute 2-DG labelling period, depending on which came first. The amount of NaCN (mg/kg) received by each group was: -6 minute group = 5.02 ± 0.44; 1 minute group = 4.37 ± 2.90; 60 minute group = 7.40 ± 0.95; 6 hour group = 9.47 ± 1.39; and 24 hour group = 6.83 ± 0.76. A pulse of [^{14}C]-2-DG was given iv -6 minutes before or 1 minute, 60 minutes, 6 hours or 24 hours after the NaCN infusion was started in order to determine LCGU. All rats were sacrificed 45 minutes after injection of 2-DG. The results are given in Table I and Figure 2. LCGU was significantly increased in the cyanide (1 minute) group (Table I, column 3) in several structures. Structures that had increases greater than 150% of control include: nucleus accumbens, lateral septum, bed nucleus striatum, globus pallidus, basolateral amygdala, central amygdala, choroid plexus, hippocampal body, CA4, substantia nigra, and interpeduncular nucleus. The structure with the highest percent increase in LCGU was corpus callosum (300% of control). This may account for the reported greater vulnerability to damage of white matter than gray matter. Sixty minutes after NaCN, LCGU was markedly reduced in all 45 regions measured, except for choroid plexus. Most regions were between 30 to 50% of control (Table I, column 4). Six and 24 hours after NaCN, LCGU was at control levels (Table I, columns 4 and 5). Thus, the expected increase in LCGU associated with a shift from aerobic to anaerobic metabolism after cyanide was of short duration. The marked reduction in LCGU found 1 hour after NaCN was dramatic and needs further exploration.

Table I. Effect of cyanide on local cerebral glucose use (μmol/100 g/min)

Brain Area	Control (N = 17)	Cyanide (N= 8) -6 minute	Cyanide (N = 8) 1 minute	Cyanide (N = 7) 60 minute	Cyanide (N = 6) 6 hour	Cyanide (N= 6) 24 hour
Olfactory Tubercle	64 ± 3	77 ± 7	85 ± 8*	24 ± 3*	59 ± 3	62 ± 5
Ventral Striatum	77 ± 4	85 ± 6	100 ± 9	33 ± 7*	75 ± 5	76 ± 3
Nucleus Accumbens	53 ± 4	64 ± 6	76 ± 7*	23 ± 4*	51 ± 3	49 ± 3
Cingulate Gyrus	86 ± 5	90 ± 7	97 ± 10	28 ± 5*	80 ± 6	79 ± 5
Frontal Cortex	79 ± 5	81 ± 6	83 ± 9	30 ± 4*	76 ± 3	77 ± 5
Frontal Cortex-Dorsal	88 ± 6	80 ± 7	84 ± 9	29 ± 4*	78 ± 7	80 ± 5
Frontal Cortex-Ventral	92 ± 7	84 ± 7	91 ± 9	35 ± 4*	82 ± 5	84 ± 6
Corpus Callosum	22 ± 2	47 ± 4*	66 ± 8*	9 ± 3*	21 ± 3	18 ± 2
Dorsolateral Caudate	88 ± 5	95 ± 7	105 ± 11	29 ± 6*	83 ± 7	86 ± 4
Ventral Pallidum	58 ± 4	55 ± 5	74 ± 10	28 ± 5*	55 ± 5	54 ± 3
Piriform Cortex	75 ± 4	79 ± 6	89 ± 10	29 ± 6*	76 ± 5	75 ± 5
Lateral Septum	43 ± 3	52 ± 6	69 ± 8*	22 ± 4*	40 ± 4	45 ± 3
Bed Nucleus Striatum	40 ± 2	56 ± 7	62 ± 7*	19 ± 4*	39 ± 4	47 ± 3
Globus Pallidus	43 ± 3	58 ± 4*	73 ± 8*	15 ± 3*	44 ± 5	49 ± 4
Basolateral Amygdala	71 ± 5	87 ± 7	98 ± 9*	27 ± 4*	65 ± 5	71 ± 5
Central Amygdala	39 ± 3	46 ± 5	58 ± 7*	16 ± 3*	40 ± 3	40 ± 3
Anteroventral Thalamus	100 ± 5	95 ± 8	109 ± 9	35 ± 5*	92 ± 7	103 ± 5
Ventrolateral Thalamus	91 ± 5	93 ± 8	107 ± 9	29 ± 3*	86 ± 7	88 ± 4
Hypothalamus	51 ± 4	52 ± 5	69 ± 6	23 ± 4*	48 ± 4	46 ± 3
Subthalamus	79 ± 5	86 ± 6	101 ± 8*	36 ± 5*	80 ± 6	87 ± 4
Mediodorsal Thalamus	90 ± 5	92 ± 7	102 ± 9	31 ± 4*	87 ± 6	94 ± 6
Laterodorsal Thalamus	91 ± 5	92 ± 7	104 ± 10	31 ± 3*	84 ± 4	93 ± 6
Mammillary Body	99 ± 6	103 ± 8	111 ± 7	41 ± 4*	99 ± 4	98 ± 5
Lateral Habenula	86 ± 5	91 ± 8	102 ± 8	43 ± 6*	78 ± 4	91 ± 7
Choroid Plexus	63 ± 4	87 ± 13	124 ± 14*	52 ± 14	47 ±4*	67 ± 7
Parietal Cortex	83 ± 5	79 ± 5	91 ± 9	28 ± 4*	73 ± 5	81 ± 6
Hippocampal Body-CA3	53 ± 4	60 ± 4	75 ± 9	28 ± 7*	50 ± 5	49 ± 6
Hippocampal Body-CA4	47 ± 3	57 ± 3*	68 ± 8*	23 ± 7*	45 ± 3	44 ± 4
Dentate Gyrus (Mol)	45 ± 3	51 ± 4	62 ± 8	17 ± 4*	45 ± 3	44 ± 4
Dorsolateral Geniculate	81 ± 3	78 ± 6	92 ± 8	28 ± 3*	76 ± 7	81 ± 6
Hippocampal-CA1-Ventral	53 ± 3	59 ± 6	77 ± 10	24 ± 4*	50 ± 3	48 ± 2
Hippocampal-CA1-Dorsal	50 ± 3	54 ± 4	68 ± 8	19 ± 4*	49 ± 5	48 ± 2
Entorhinal Cortex	62 ± 4	62 ± 6	83 ± 10	27 ± 8*	55 ± 4	55 ± 2
Anterior Pretectum-Thalamus	90 ± 5	82 ± 7	102 ± 8	40 ± 4*	82 ± 6	88 ± 6
Substantia Nigra	54 ± 3	56 ± 5	87 ± 7*	28 ± 5*	51 ± 2	51 ± 2
Substantia Nigra-Hi	62 ± 3	69 ± 4	96 ± 6*	33 ± 5*	58 ± 2	61 ± 3
Substantia Nigra-Lo	50 ± 3	52 ± 6	81 ± 8*	25 ± 4*	45 ± 2	46 ± 2
Interpeduncular Nucleus	86 ± 6	86 ± 6	118 ± 13	47 ± 7*	95 ± 5	81 ± 3
Medial Geniculate	96 ± 5	86 ± 6	102 ± 9	31 ± 2*	91 ± 4	103 ± 7
Superior Colliculus	74 ± 4	73 ± 5	87 ± 8	36 ± 4*	73 ± 4	74 ± 5
Lateral Lemniscus	88 ± 5	88 ± 7	104 ± 7	41 ± 4*	91 ± 6	92 ± 5
Presubiculum	79 ± 4	78 ± 7	92 ± 7	25 ± 3*	82 ± 5	73 ± 5
Inferior Colliculus	118 ± 6	108 ± 10	114 ± 9	58 ± 3*	116 ± 4	129 ± 3
Vermis (Dorsal Lobule)	49 ± 2	52 ± 5	65 ± 7	24 ± 4*	53 ± 4	49 ± 3
Vermis (Lobule 1)	102 ± 6	103 ± 10	109 ± 7	45 ± 7*	101 ± 7	98 ± 1

Data expressed as means ± S.E.

*Significantly different from control ($p < 0.05$).

To determine if the suppression of LCGU was a direct effect of cyanide or an indirect effect, a microdialysis fiber was implanted into the right striatum in order that cyanide could be directly applied to a given brain region. Approximately 24 hours after surgery, rats were divided into 3 groups and the microdialysis fiber was perfused with saline (control group), 2 mM or 10 mM NaCN at a flow rate of 2 µl/min for 60 minutes. A pulse of [^{14}C]-2-DG was given iv after 15 minutes of saline or NaCN perfusion. Saline or NaCN perfusion was continued and all rats were sacrificed 45 minutes after 2-DG. The rates of LCGU on the fiber side and contralateral side are given in Table II. Perfusion with 2 mM NaCN did not produce any significant changes on either the fiber side or the contralateral side, whereas perfusion with 10 mM NaCN reduced LCGU values in every structure measured on both the fiber side and the contralateral side. The reduction was significant in 13/45 structures evaluated on the contralateral side and in 23/45 structures measured on the fiber side. The degree of reduction was usually somewhat greater on the fiber side than the contralateral side. Most structures on the fiber side were reduced to about 50% of control values irrespective of the distant from the fiber. These results strongly suggest that exposure of the brain to cyanide (at least the striatum) triggers a response that reduces brain metabolism throughout the brain. Using this same method of exposure Yamazaki and co-workers (1992) have demonstrated dopamine levels in the perfusate markedly increased with NaCN perfusion. These studies provide evidence that cyanide reduces brain metabolism via an indirect effect. The increase in dopamine may be a possible candidate that results in a shut down of brain activity.

Microdialysis studies: To further our understanding of changes in brain metabolism during cyanide exposure, a microdialysis fiber was implanted into the right piriform cortex. In these studies, rats were infused intravenously with either saline or cyanide as described above. In addition, the fiber was perfused with KRB at a rate of 8 µl/min. Basal perfusate levels of

LOCAL CEREBRAL GLUCOSE UTILIZATION

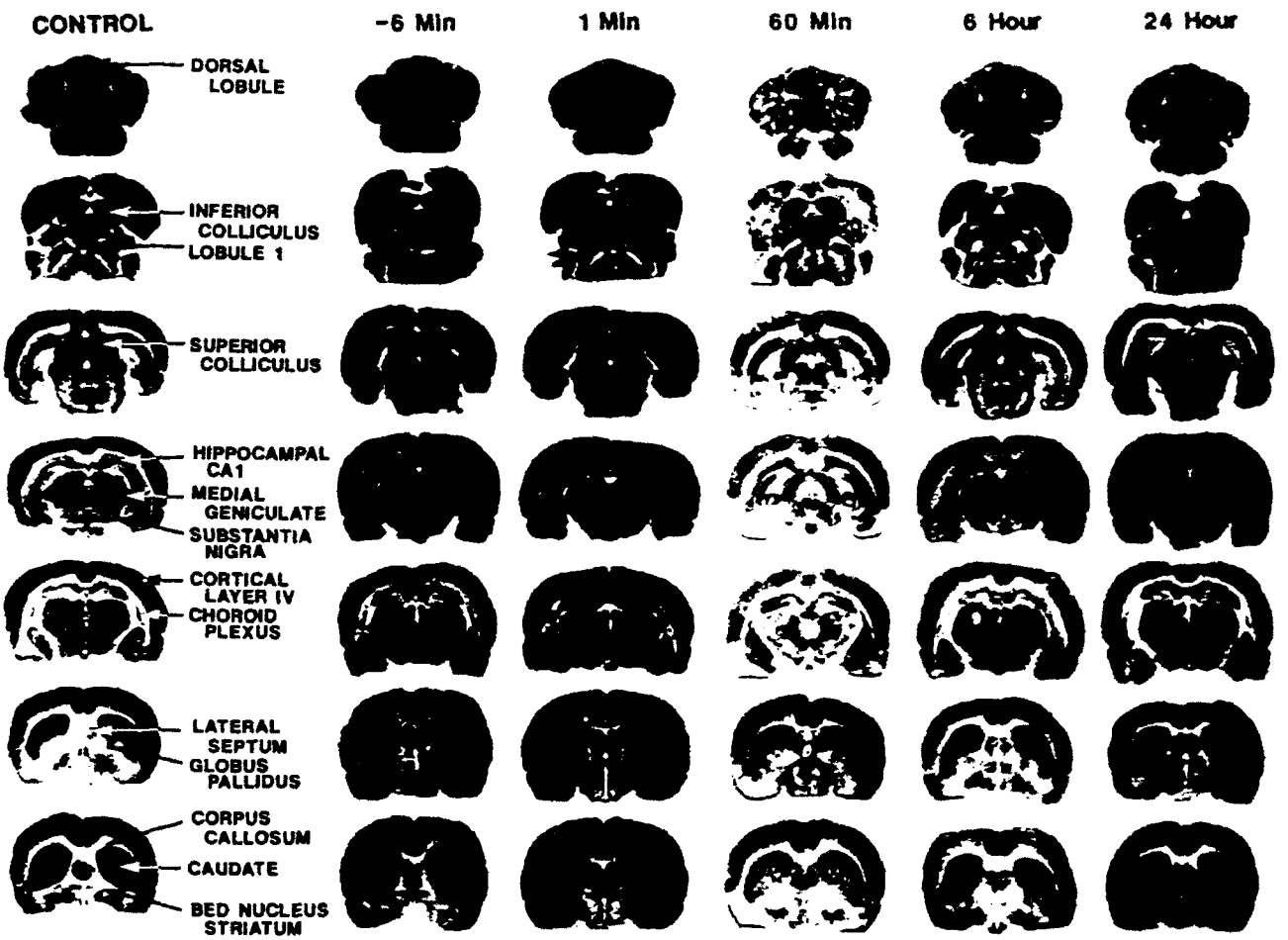

Figure 2. Representative LCGU autoradiograms. Groups include: Control (N=17); CN -6 min. (N=8); CN 1 min. (N=8); CN 60 min. (N=7); CN 6 hr. (N=6) and CN 24 hr. (N=6). The time indicates when 2-DG was given with respect to initiation of NaCN infusion.

Table II. Effect of cyanide on local cerebral glucose use (μmol/100 g/min) when delivered directly to the striatum via microdialysis.

Brain Area	Contralateral Side			Fiber Side		
	Vehicle (N = 5)	CN 2 mM (N= 6)	CN 10 mM (N = 7)	Vehicle (N = 5)	CN 2 mM (N = 6)	CN 10 mM (N = 7)
Olfactory Tubercle	67 ± 11	65 ± 9	37 ± 10	61 ± 10	55 ± 9	34 ± 10
Ventral Striatum	69 ± 1	72 ± 8	45 ± 1	68 ± 11	58 ± 6	36 ± 9
Nucleus Accumbens	44 ± 4	42 ± 6	24 ± 6*	42 ± 4	47 ± 7	23 ± 7*
Cingulate Gyrus	78 ± 11	89 ± 11	50 ± 14	73 ± 12	81 ± 12	44 ± 14
Frontal Cortex	70 ± 13	71 ± 9	40 ± 10	58 ± 13	49 ± 6	27 ± 7
Frontal Cortex-Dorsal	70 ± 11	71 ± 9	40 ± 11	60 ± 12	48 ± 6	27 ± 7
Frontal Cortex-Ventral	66 ± 10	66 ± 10	40 ± 10	59 ± 12	51 ± 9	27 ± 8
Corpus Callosum	20 ± 5	18 ± 2	10 ± 3	23 ± 5	20 ± 3	9 ± 2*
Dorsolateral Caudate	74 ± 14	75 ± 9	44 ± 11	66 ± 12	64 ± 8	32 ± 7
Ventral Pallidum	53 ± 10	46 ± 11	23 ± 6*	55 ± 9	45 ± 8	23 ± 5*
Piriform Cortex	57 ± 11	54 ± 9	31 ± 6	50 ± 13	48 ± 9	25 ± 5
Lateral Septum	37 ± 9	42 ± 8	25 ± 6	36 ± 10	40 ± 7	26 ± 5
Bed Nucleus Striatum	58 ± 10	39 ± 4	26 ± 5*	53 ± 10	37 ± 5	27 ± 7
Globus Pallidus	31 ± 5	34 ± 5	17 ± 4	32 ± 3	32 ± 5	15 ± 3*
Basolateral Amygdala	59 ± 6	59 ± 6	27 ± 6*	55 ± 7	59 ± 6	25 ± 5*
Central Amygdala	33 ± 2	33 ± 5	15 ± 3*	30 ± 2	35 ± 7	12 ± 1*
Anteroventral Thalamus	81 ± 11	90 ± 9	51 ± 14	77 ± 10	89 ± 9	50 ± 12
Ventrolateral Thalamus	75 ± 11	78 ± 5	44 ± 12	70 ± 11	64 ± 10	30 ± 9*
Hypothalamus	45 ± 6	42 ± 5	26 ± 8	43 ± 4	46 ± 8	23 ± 6*
Subthalamus	62 ± 9	66 ± 8	34 ± 9*	55 ± 7	63 ± 8	27 ± 8*
Mediodorsal Thalamus	73 ± 13	78 ± 7	44 ± 13	67 ± 10	77 ± 8	35 ± 12
Laterodorsal Thalamus	76 ± 9	61 ± 7	43 ± 12	65 ± 8	72 ± 10	35 ± 12
Mammillary Body	78 ± 14	93 ± 10	49 ± 13	77 ± 11	92 ± 10	46 ± 11
Lateral Habenula	71 ± 11	75 ± 10	39 ± 10	73 ± 9	73 ± 13	36 ± 8*
Choroid Plexus	34 ± 4	34 ± 6	17 ± 4*	33 ± 4	34 ± 6	16 ± 3*
Parietal Cortex	75 ± 12	75 ± 11	36 ± 9*	57 ± 6	61 ± 10	32 ± 9
Hippocampal Body-CA3	54 ± 10	48 ± 6	27 ± 8	42 ± 6	47 ± 9	22 ± 6*
Hippocampal Body-CA4	43 ± 9	48 ± 6	26 ± 9	35 ± 4	44 ± 7	22 ± 6
Dentate Gyrus (Mol)	42 ± 8	38 ± 5	24 ± 7	37 ± 5	37 ± 8	19 ± 5*
Dorsolateral Geniculate	64 ± 10	63 ± 8	38 ± 12	63 ± 8	58 ± 8	29 ± 10*
Hippocampal-CA1-Ventral	48 ± 9	45 ± 4	28 ± 7	45 ± 7	40 ± 5	20 ± 6*
Hippocampal-CA1-Dorsal	43 ± 9	38 ± 5	24 ± 8	39 ± 4	35 ± 4	19 ± 6*
Entorhinal Cortex	52 ± 7	50 ± 6	29 ± 8	40 ± 4	47 ± 8	26 ± 8
Anterior Pretectum-Thalamus	75 ± 11	73 ± 9	39 ± 9*	71 ± 11	69 ± 9	35 ± 9*
Substantia Nigra	45 ± 6	44 ± 3	23 ± 7*	39 ± 6	39 ± 6	21 ± 5*
Substantia Nigra-Hi	46 ± 7	39 ± 3	21 ± 7*	35 ± 6	35 ± 5	20 ± 6
Substantia Nigra-Lo	51 ± 11	48 ± 5	28 ± 9	46 ± 8	43 ± 6	26 ± 6
Interpeduncular Nucleus	66 ± 11	72 ± 8	45 ± 11	81 ± 13	68 ± 8	40 ± 11*
Medial Geniculate	82 ± 10	79 ± 9	44 ± 10*	78 ± 12	72 ± 10	35 ± 8*
Superior Colliculus	59 ± 10	67 ± 8	34 ± 9	51 ± 7	64 ± 7	27 ± 7*
Lateral Lemniscus	77 ± 14	78 ± 11	45 ± 11	75 ± 11	79 ± 13	39 ± 10*
Presubiculum	66 ± 13	69 ± 9	41 ± 12	57 ± 12	65 ± 10	33 ± 9
Inferior Colliculus	121 ± 11	118 ± 11	76 ± 15*	115 ± 11	124 ± 1	72 ± 14*
Vermis (Dorsal Lobule)	42 ± 9	43 ± 7	26 ± 6	39 ± 7	43 ± 7	23 ± 7
Vermis (Lobule 1)	102 ± 16	87 ± 13	60 ± 17	101 ± 14	90 ± 12	57 ± 15

Data expressed as means ± S.E.

*Cyanide Significantly different from vehicle ($p < 0.05$).

lactate (ca 100 μM) were determined prior to cyanide exposure (see Figures 3 and 4). Cyanide infusion and 2-DG injection were given at times indicated in Figures 3 and 4. Specifically, 150 μCi/kg of [^{14}C]-2-DG was given either 15 (Figure 3) or 60 (Figure 4) minutes after initiation of NaCN infusion. The control group received saline infusion throughout the experiment. After the injection of 2-DG, lactate (Figures 3 and 4) and [^{14}C]-label (Figure 5) were monitored in the perfusate. Glucose (Figure 6) and [^{14}C]-label (Figure 7) were monitored in the plasma. The animals were sacrificed 45 minutes after 2-DG injection. After the start of NaCN infusion, perfusate lactate levels increased 4- to 5-fold over basal levels (Figures 3 and 4). This is further evidence of a shift from aerobic to anaerobic metabolism. The fact that perfusate lactate levels rapidly decline at a time when LCGU is low (see Table I and Figure 4; cyanide--60 minute--group) suggests that both anaerobic and aerobic brain metabolism have decreased. An alternate explanation for low LCGU after 60 minutes of cyanide exposure would be that cyanide is inhibiting the transport of 2-DG into the brain, thus falsely indicating a decrease in LCGU. This was ruled out by measuring the amount of [^{14}C]-label in the extracellular fluid. As seen in Figure 5 (cyanide--60 minute--group), [^{14}C]-label is actually above control when LCGU is low. Thus, 2-DG is getting into the brain but is not being used after 60 minutes of cyanide exposure. Further, the decline in plasma [^{14}C]-label (Figure 7) was slowed after cyanide infusion and appeared to be related to the marked hyperglycemia produced by cyanide (Figure 6). This was most prominent in the cyanide (15 minute) group, the group where plasma was collected during the cyanide infusion.

These results support the hypothesis that cyanide causes a shift in brain from aerobic to anaerobic metabolism; however, the short duration of the LCGU increase indicates that a marked depression of both aerobic and anaerobic metabolism rapidly follows NaCN exposure. We had earlier suggested that sublethal cyanide leads to increased K^+ throughout the brain within minutes

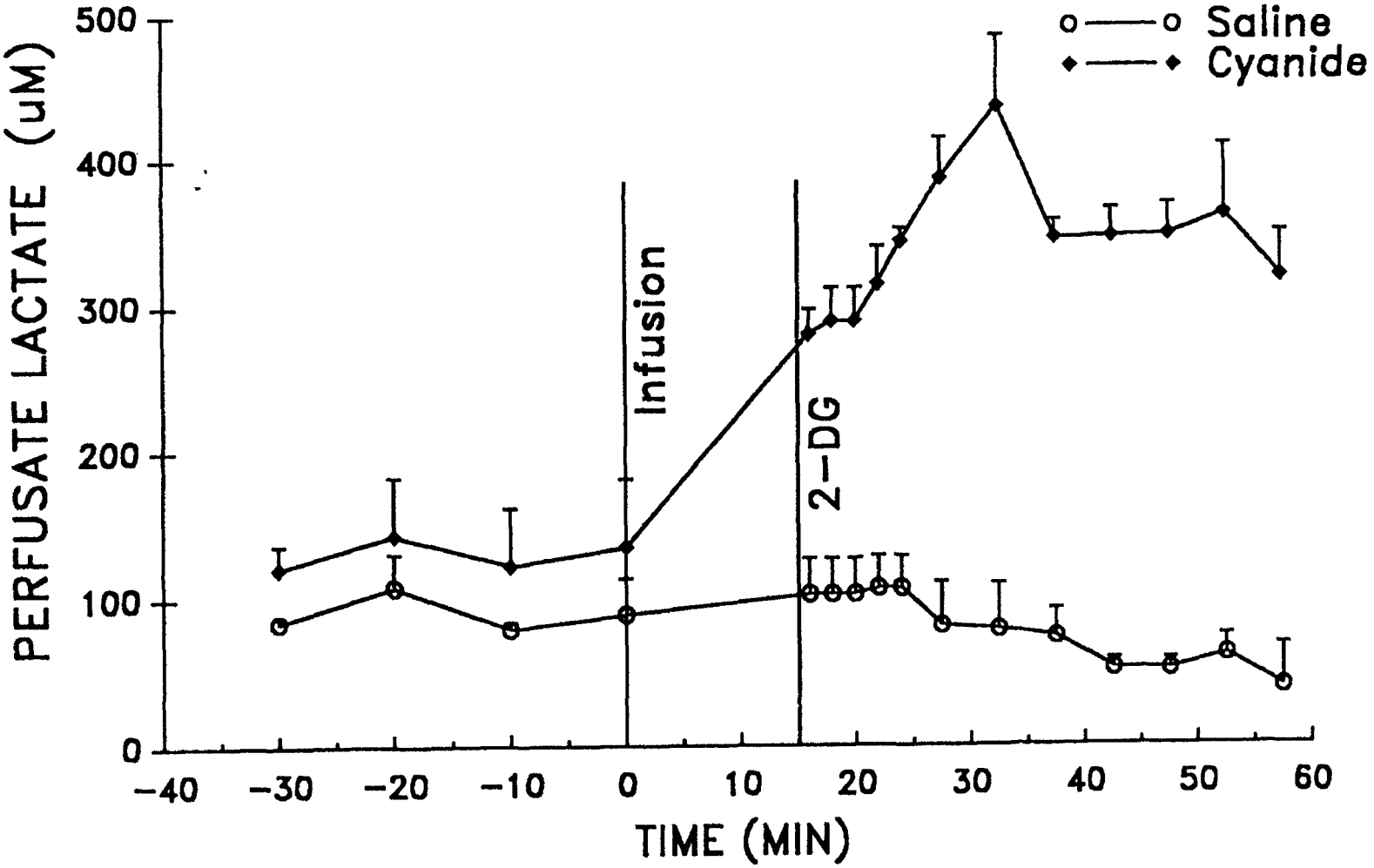

Figure 3. Concentration of lactate in microdialysis perfusate after cyanide exposure. A microdialysis fiber was implanted into the right piriform cortex. Intravenous saline infusion was initiated at -30 minutes and NaCN infusion (20 µl/min; 5 mg/ml) was initiated at time marked (infusion) and given for 60 minutes as described in the text. The microdialysis fiber was perfused with KRB at 8 µl/min and lactate was measured in the perfusate. [^{14}C]-2-DG was injected 15 minutes after the infusion initiation. The rats were sacrificed 45 minutes after injection of 2-DG. Control, N = 4; cyanide, N = 3. Data were analyzed by repeated measures--ANOVA. Prior to cyanide exposure basal levels were not significantly greater than control; $p < 0.05$.

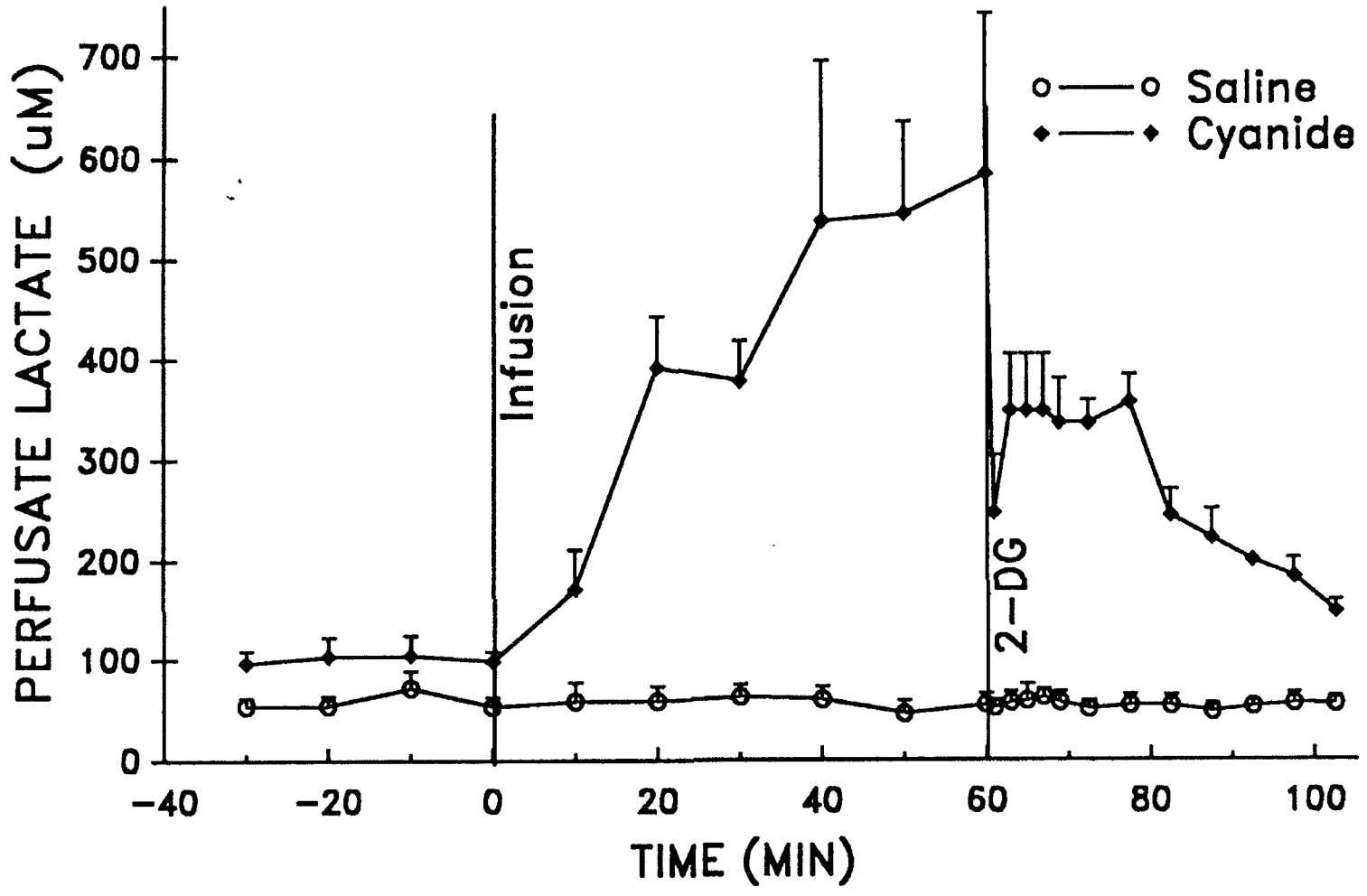

Figure 4. Concentration of lactate in microdialysis perfusate after cyanide exposure. A microdialysis fiber was implanted into the right piriform cortex. Intravenous saline infusion was initiated at -30 minutes and NaCN infusion (20 µl/min; 5 mg/ml) was initiated at time marked (infusion) and given for 60 minutes as described in the text. The microdialysis fiber was perfused with KRB at 8 µl/min and lactate was measured in the perfusate. [^{14}C]-2-DG was injected 60 minutes after the infusion initiation. The rats were sacrificed 45 minutes after injection of 2-DG. Control, N = 5; cyanide, N = 4. Data were analyzed by repeated measures--ANOVA. Prior to cyanide exposure basal levels were not significantly greater than control; $p < 0.05$.

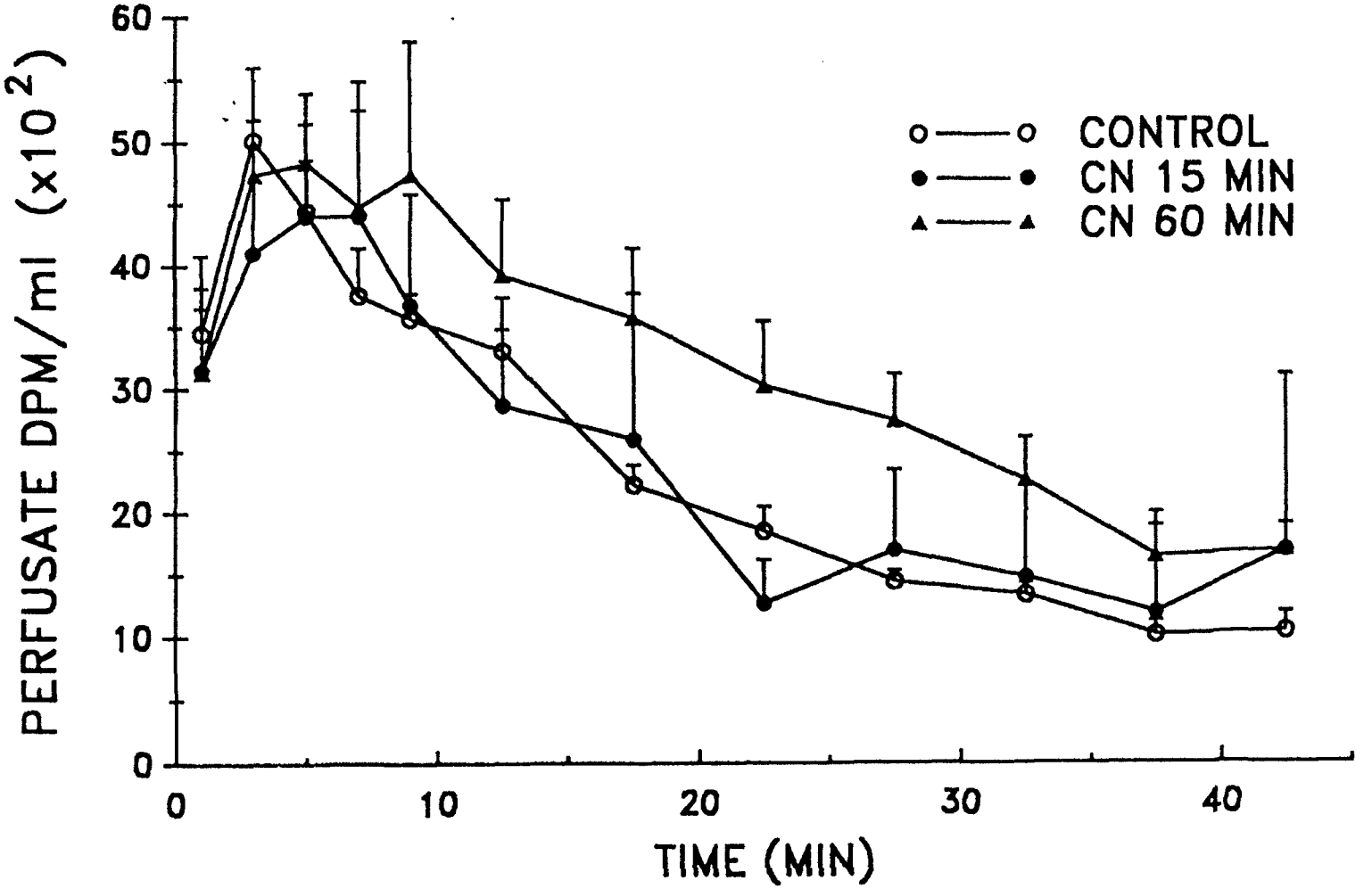

Figure 5. [^{14}C]-radioactivity in microdialysis perfusate after cyanide exposure. Rats were treated as described in Figures 3 and 4. [^{14}C]-radioactivity was determined in the perfusate. Data were analyzed by repeated measures--ANOVA. Perfusate levels did not differ significantly between the three treatments ($p = 0.42$). After the initial rise, DPM values decreased over time ($p < 0.0001$). The rate of decline was not affected by treatment ($p = .90$).

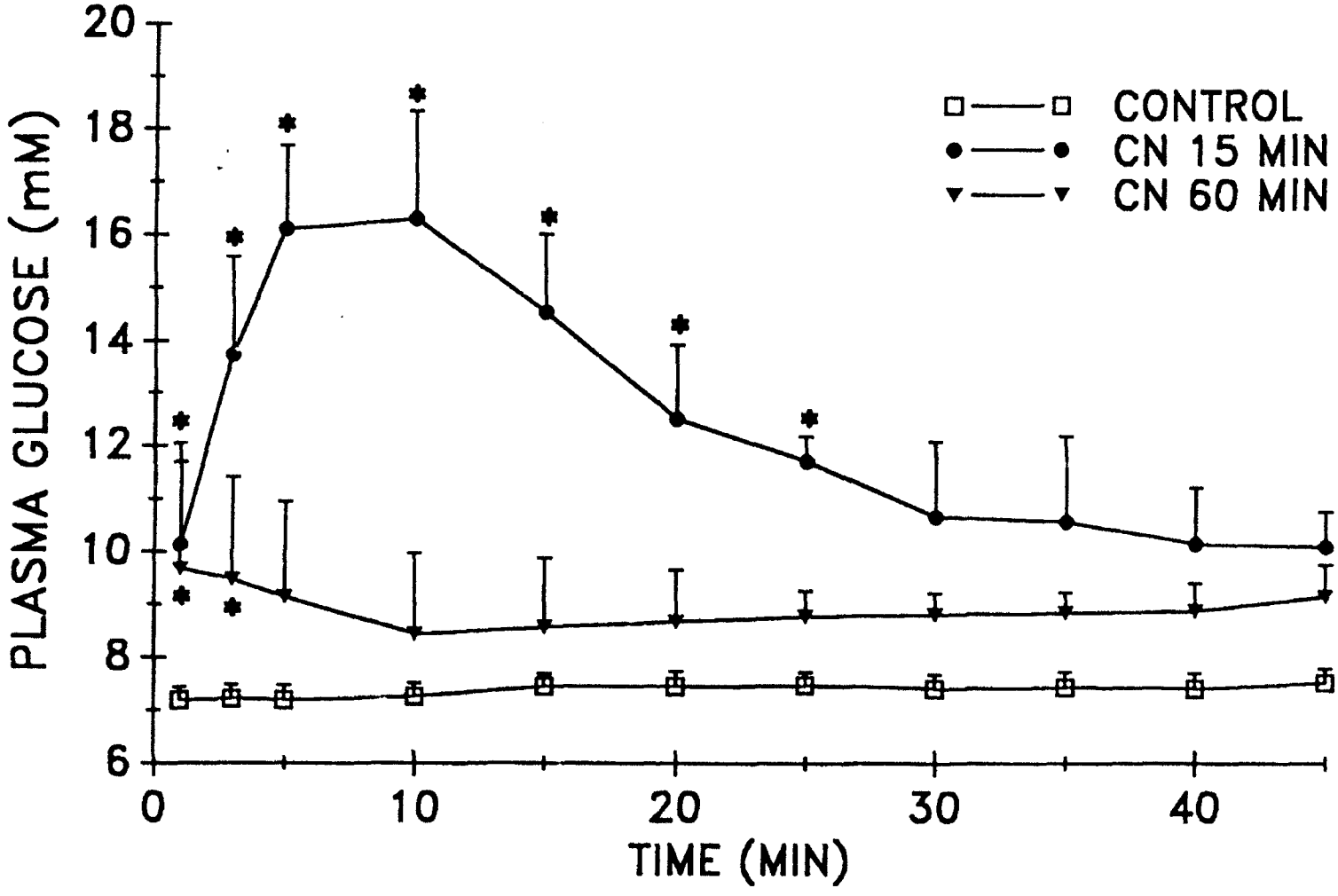

Figure 6. Concentration of glucose in the plasma after cyanide exposure. Rats were treated as described in Figures 3 and 4. Glucose levels were determined in the plasma. Data were analyzed by repeated measures--ANOVA. The treatment, time and treatment x time effects are statistically significant at the 0.05 level. When averaged over all times, the mean glucose concentration for CN 15 minute is greater than CN 60 minute or control treatments ($p = 0.0079$ and $p = 0.0003$, respectively). The overall mean for CN 60 minute is marginally greater than the glucose concentration mean for control treatment ($p = 0.0549$). * indicates that glucose concentration is greater than control at corresponding times ($p < 0.05$).

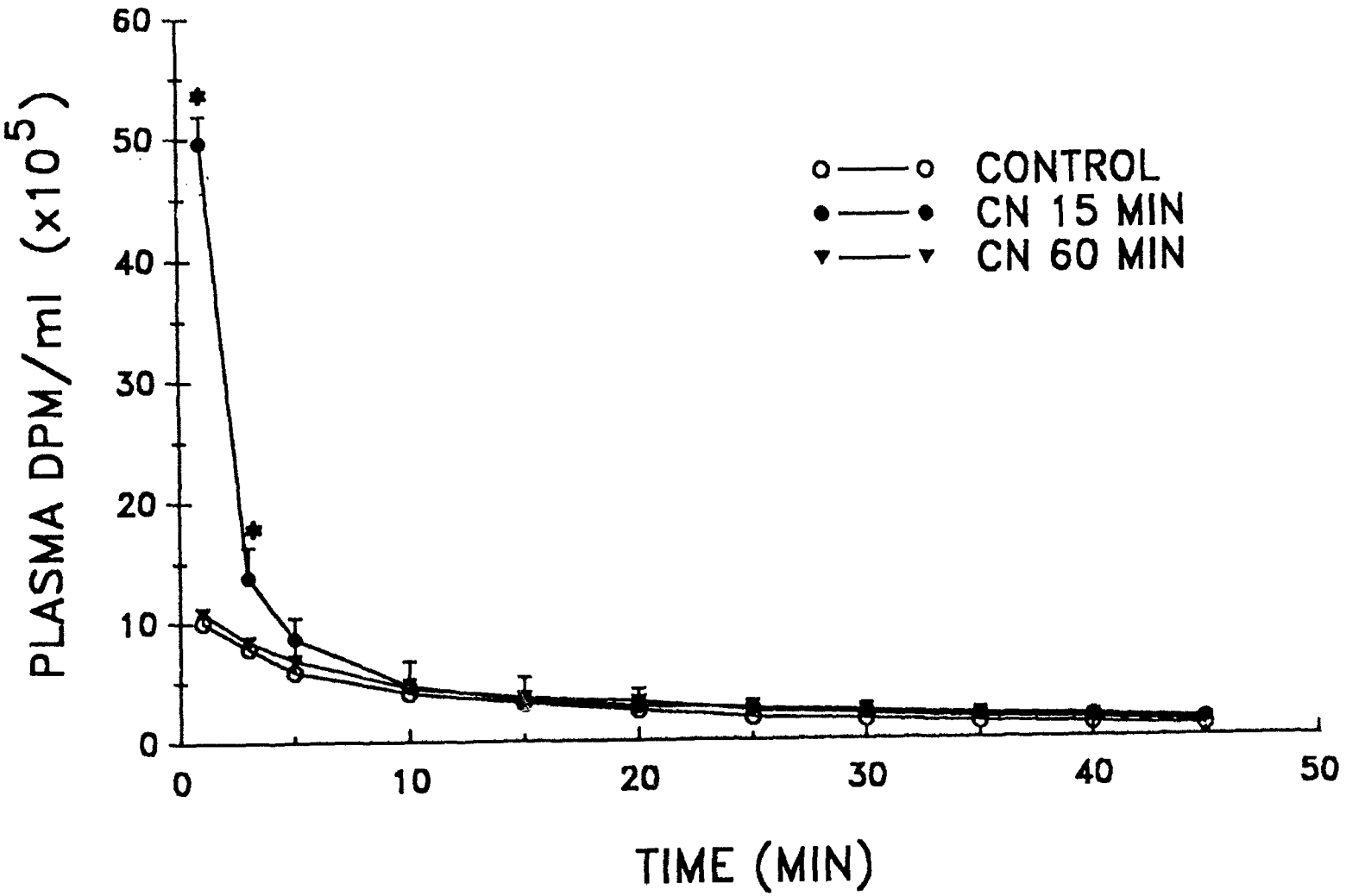

Figure 7. [^{14}C)-radioactivity in plasma after cyanide exposure. Rats were treated as described in Figures 3 and 4. [^{14}C]-radioactivity was determined in the plasma. Data were analyzed by repeated measures--ANOVA. There is a statistically significant decrease in plasma DPM over time (for all treatments, $p < 0.0001$). Additionally, the treatment x time interaction is significant. Inspection of the cell-means indicates that CN 15 minute is greater (*) than CN 60 minute at 1 and 3 minute post 2-DG and greater than control at 1, 3 and 5 minute ($p < 0.05$). Differences in the three treatments at 10 minute and later post 2-DG injection are not statistically significant (all p values > 0.20).

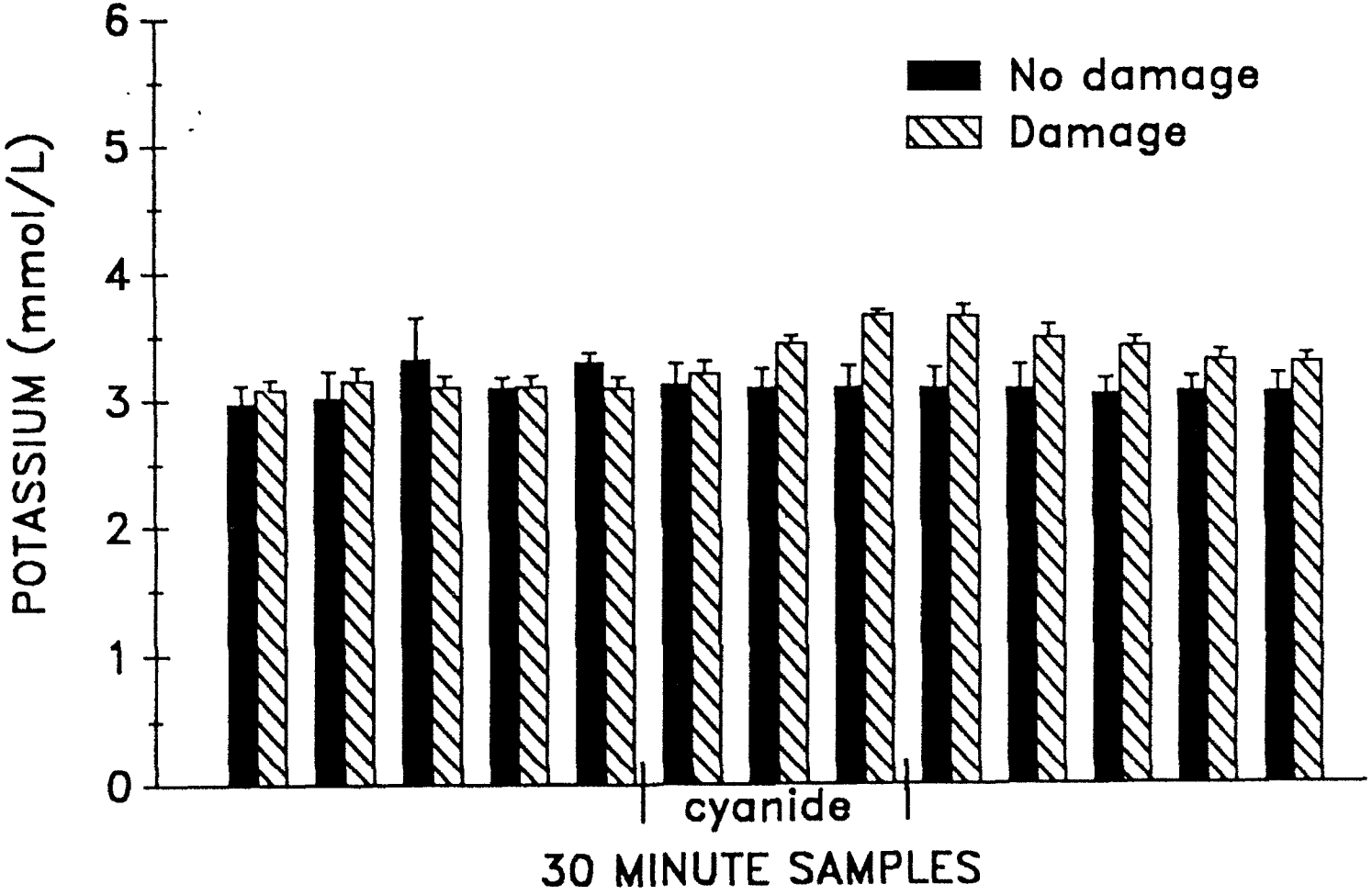

Figure 8. Concentration of potassium (mM) in microdialysis perfusates before, during and after cyanide exposure. A microdialysis fiber was implanted into the right piriform cortex. Rats were given intravenous saline or NaCN as stated in methods. NaCN was given for 90 minutes at times indicated on the graph. N = 3 no damage group; N = 2 damage group. Damage was assessed by qualitative inspection of 2-DG autoradiograms.

after exposure and the high K^+ caused a marked depression in cerebral activity. We have determined the K^+ level in the extracellular fluid (ECF) at various time intervals after NaCN by intracerebral microdialysis. The extracellular K^+ (see Figure 8) does not change significantly during the time of depressed cerebral activity and thus does not account for the cerebral depression. Na^+ levels did not change before, during or after NaCN exposure (data not shown). Aitken and Braitman (1989) reported that cyanide inhibits neural and synaptic function in hippocampal slices. They suggest that cyanide has a direct affect on neurons not mediated by its inhibition of metabolism. We further suggest that this effect can influence brain activity at sites remote from cyanide exposure (see Table II) possibly via substance that can traverse freely through the ECF.

In the next set of microdialysis studies, a microdialysis fiber was placed in the right piriform cortex and perfusate was collected before, during and after NaCN exposure. NaCN exposure was as described in methods. In some situations saline instead of NaCN was infused as an additional control. In some rats the 2-DG procedure was performed at the end of the experiment to assess if brain damage had occurred. There were four separate studies done to measure 1) acid products of anaerobic metabolism, 2) brain monoamines and metabolites, 3) redox-active substances, and 4) brain amino acids.

The perfusate concentration of both lactate and pyruvate increased greater than 4-fold during cyanide exposure (see Figures 9 and 10). Basal levels of lactate were high (ca 1 mM), and increased dramatically (3- to 10-fold) following events that stimulate glycolysis such as ischemia in the brain (Kuhr *et al.*, 1988). Therefore, the regulation of intracellular and extracellular lactate levels are important in restoration of cell function after metabolic insults.

Kuhr *et al.* (1988) have provided evidence for a carrier-mediated transport of lactate in the brain. This transport system only functions when energy supplies can maintain membrane integrity and function. Moreover, lactate is not cleared from brain tissue by the vascular system as it is in

muscle tissue, but in brain, lactate is recycled to pyruvate. Since the metabolic rate is quite different between cells (glia vs. neurons), there may be a rapid transfer of lactate between cells such that the large reservoir of energy present in accumulated lactate is not wasted, but instead utilized by other cells in the brain. It is crucial that brain activity is shut down during cyanide exposure prior to extensive depletion of energy reserves because the anaerobic accumulation of intracellular lactate could lower pH and cause devastating neurotoxicity.

The effects of cyanide exposure on monoamine metabolism is still unresolved (see review by Borkowitz *et al.*, 1992). As mentioned previously (Oguchi, personal communication), delivery of NaCN (2 mM or 10 mM) to the rat striatum produced a rapid rise, then fall of dopamine followed by a delayed reduction in DOPAC and homovanillic acid (HVA). In our study, we were unable to find meaningful changes in norepinephrine, dopamine or serotonin. This is probably due to the use of fibers that contained a stainless steel wire for support. Subsequently, we found that these fibers produce extensive amounts of hydrogen peroxide when exposed to perfusion media and even more when exposed to extracellular fluid. Commercial fibers also contain a steel wire support but they are treated with a reducing substance. However, these commercial fibers destroy all hydrogen peroxide formed and therefore are not useful to measure redox-active substance in perfusates. In this study, we observed that the acid metabolites of monoamines increased dramatically and remained elevated for several hours after NaCN infusion was stopped. The results are shown in Figure 11 (HVA), Figure 12 (DOPAC) and Figure 13 (HIAA).

There are marked increases in extracellular dopamine in the striatum and dorsal hippocampus during cerebral ischemia (Bhardwaj *et al.*, 1990; Slivka *et al.*, 1988; Brannan *et al.*, 1987). In the above mentioned studies, extracellular concentrations of HVA and DOPAC did not change significantly or were slightly reduced. This might suggest that dopamine released during ischemia is not metabolized because of failure of dopamine re-uptake mechanisms or metabolic enzyme failure.

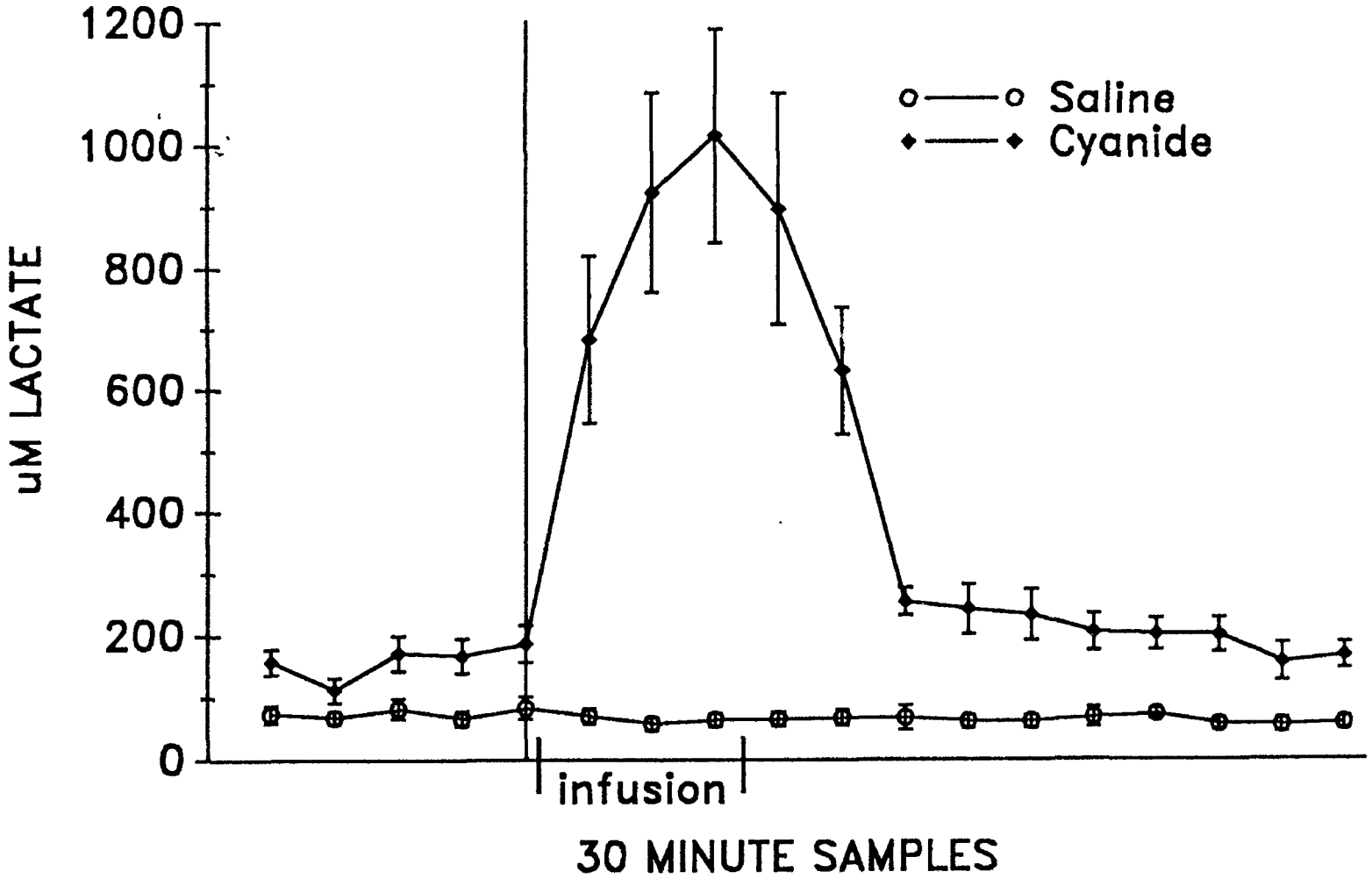

Figure 9. Concentration of lactate (μM) in microdialysis perfusates before, during and after NaCN exposure. A microdialysis fiber was implanted into the right piriform cortex. Rats were given intraveneous saline or NaCN as stated in methods. NaCN was given for 90 minutes at times indicated on the graph. N = 5, saline group; N = 5, cyanide group.

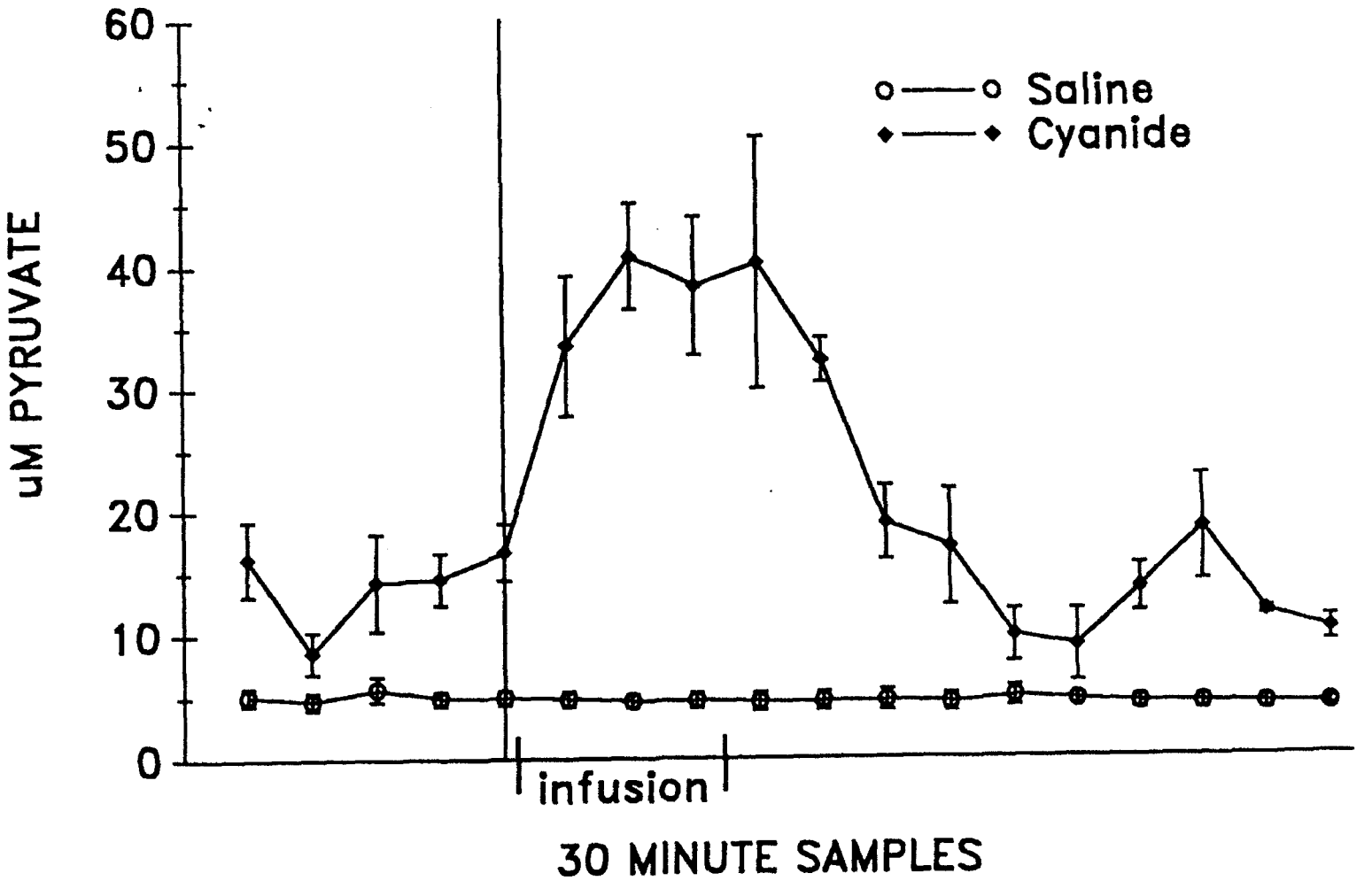

Figure 10. Concentration of pyruvate (μM) in microdialysis perfusates before, during and after cyanide exposure. A microdialysis fiber was implanted into the right piriform cortex. Rats were given intraveneous saline or NaCN as stated in methods. NaCN was given for 90 minutes at times indicated on the graph. N = 5, saline group; N = 5, cyanide group.

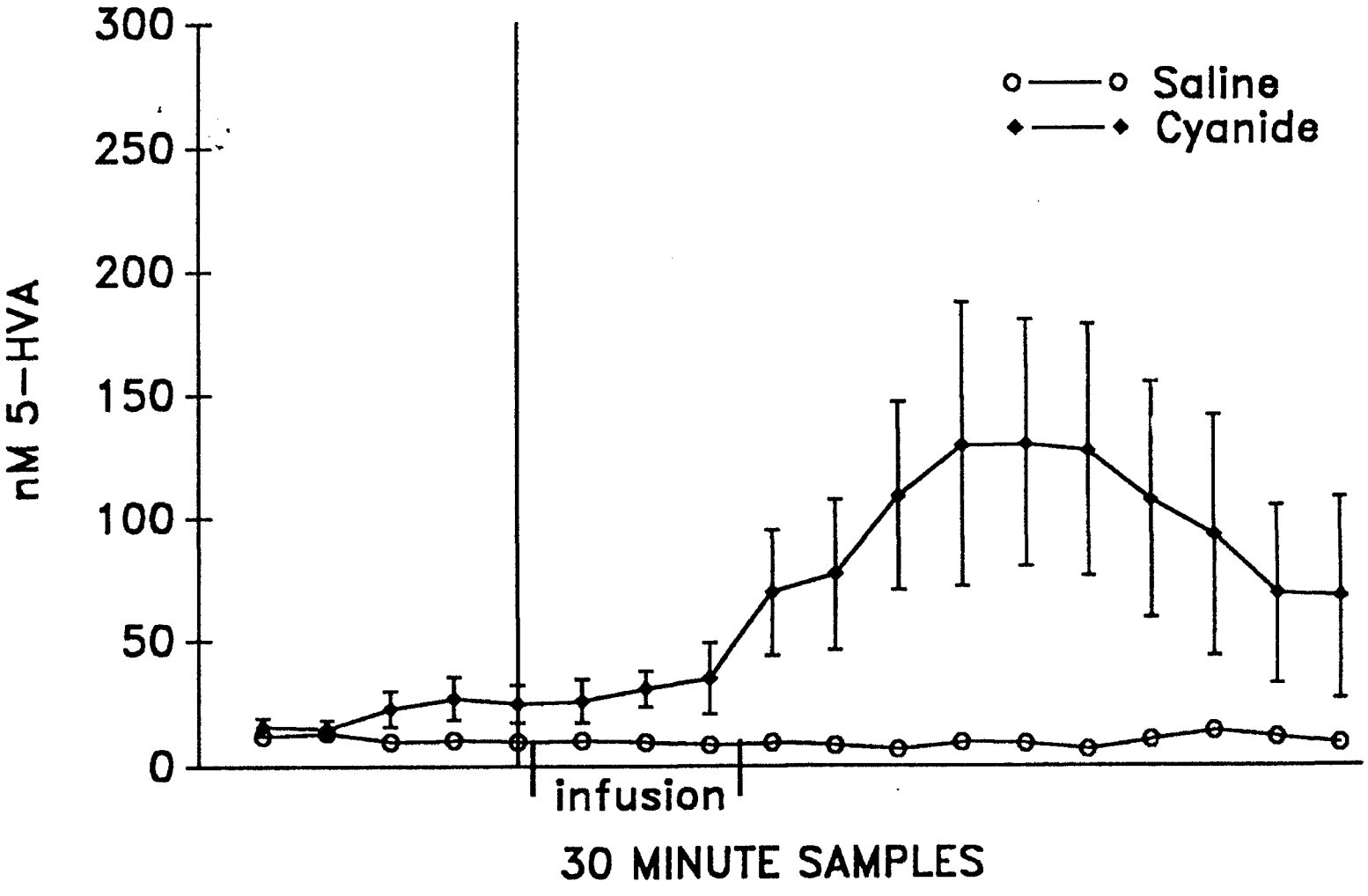

Figure 11. Concentration of HVA (nM) in microdialysis perfusates before, during and after cyanide exposure. A microdialysis fiber was implanted into the right piriform cortex. Rats were given intravenous saline or NaCN as stated in methods. NaCN was given for 90 minutes at times indicated on the graph. N = 5, cyanide exposure; N = 1, saline exposure.

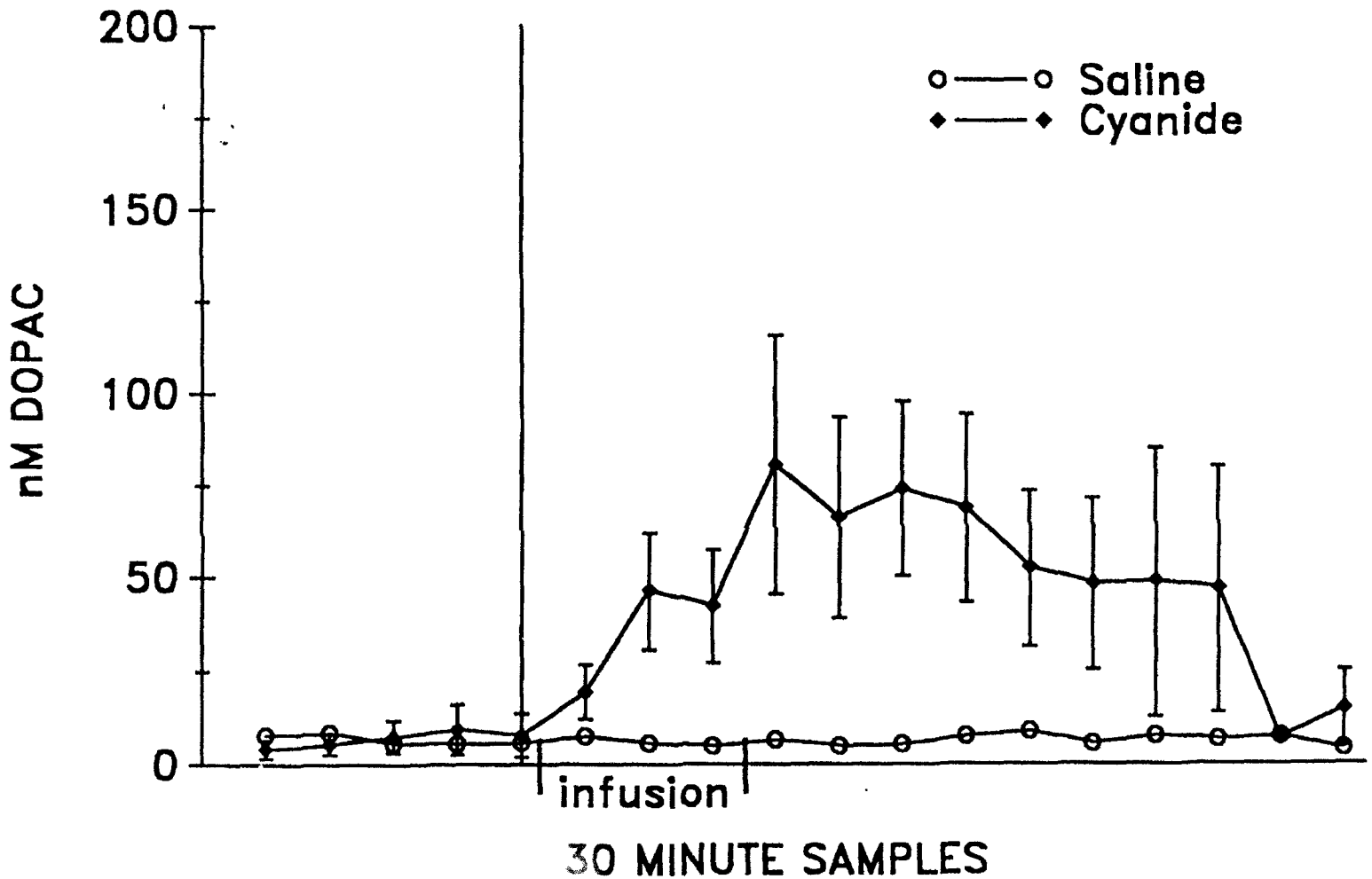

Figure 12. Concentration of DOPAC (nM) in microdialysis perfusates before, during and after cyanide exposure. A microdialysis fiber was implanted into the right piriform cortex. Rats were given intraveneous saline or NaCN as stated in methods. NaCN was given for 90 minutes at times indicated on the graph. N = 5, cyanide exposure; N = 1, saline exposure.

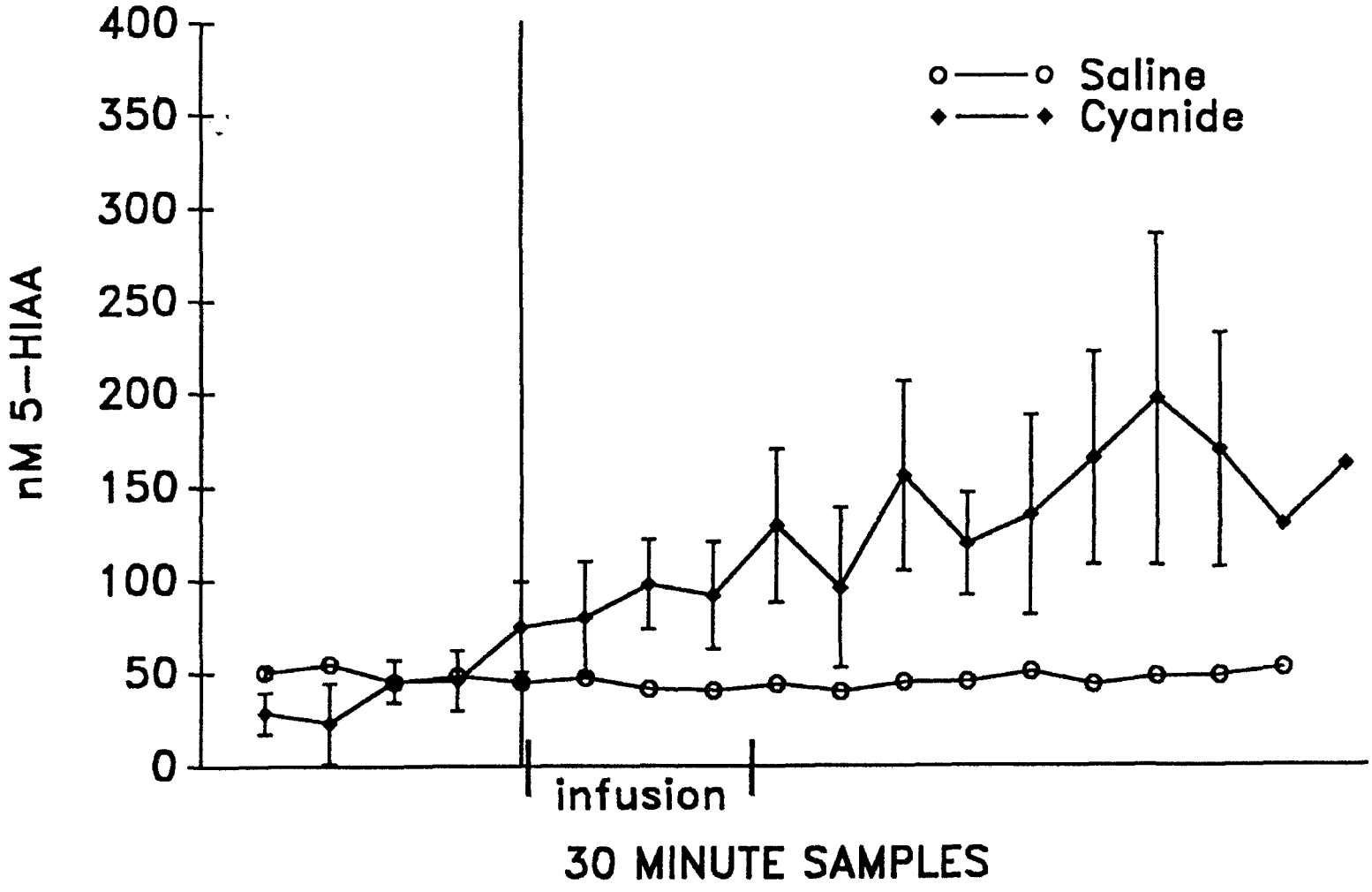

Figure 13. Concentration of HIAA (nM) in microdialysis perfusates before, during and after cyanide exposure. A microdialysis fiber was implanted into the right piriform cortex. Rats were given intraveneous saline or NaCN as stated in methods. NaCN was given for 90 minutes at times indicated on the graph. N = 5, cyanide exposure; N = 1, saline exposure.

However, studies by the same authors have shown that tissue levels of HVA and DOPAC do increase after ischemia (Weinberger and Nieves-Rosa, 1987). Thus, it appears that monoamine metabolism does proceed following ischemia, but that the acid metabolites formed remain in the metabolizing cells and are not released into the ECF. Thus, our own studies (Figures 11-13) are compatible with the notion that large amounts of monoamines are released during cyanide exposure, but they are probably destroyed by the hydrogen peroxide formed in the perfusates because of the steel in the fiber assembly. Monoamines enter cells by re-uptake processes and are metabolized to acid metabolites (e.g. HVA, DOPAC, HIAA). Since brain activity is markedly reduced (see 2-DG studies), the metabolites are stored in metabolizing cells and then slowly released as brain activity is restored. The question that remains unresolved is whether or not the massive release of monoamines contribute to the suppression of brain activity associated with NaCN exposure.

Our studies on neurotoxic substances (e.g. soman, kainic acid (KA), cyanide (CN), etc.) have led us to propose that free radicals produced in response to the toxic agents exceed the brain's antioxidant defenses which result in dysfunction and neuropathology. Most neurotoxic chemicals initiate their responses by binding to one or more specific receptors. This initiation event sets in motion a cascade of events that converge on the brain's redox status. When the antioxidant reserves are depleted the outcome is brain dysfunction or damage. Thus, we propose that pharmacological compounds that either increase the antioxidant potential or decrease the rate of oxidation would provide broad spectrum protection against numerous neurotoxic substances. Moreover, they could be given after initial exposure to the neurotoxic agent but before the radicals induce damaging chain reactions of lipid peroxidation. But first, the biochemical systems (i.e., biomarkers) involved in toxin-induced oxidations and the protective antioxidant responses must be identified. Our recent studies and the rapidly expanding literature in the field strongly implicate oxygen free radicals and

nitric oxide as key compounds in oxidative tissue dysfunction and ascorbate, α-tocopherol, urate, and enzymes (e.g. superoxide dismutase, catalase, glutathione peroxidase, etc.) as the key antioxidants.

Thus, we studied redox-active substances in the ECF sampled by microdialysis before, during and after NaCN exposure. A microdialysis fiber was implanted into the right piriform cortex. The fiber was perfused with Ringer's perfusion media before, during and after NaCN exposure. Alternate perfusate samples (15 and 20 min) were analyzed by HPLC for ascorbate and urate (Figures 14 and 15) and chemiluminescence, respectively without (Figure 16) and with catalase (Figure 17) treatment. We spent considerable effort in the design of inert microdialysis fibers which would not form hydrogen peroxide when exposed to perfusion media. We were able to design an inert fiber prepared from fused silica and teflon tubing. With the use of these fibers, ascorbate levels (Figure 14) increased at least 5-fold immediately after NaCN exposure and urate levels (Figure 15) increased slightly. Results from other studies in our laboratory indicate that ascorbate levels increase rapidly after brain insults (e.g. trauma, seizures) and the increase is independent of brain activity whereas urate levels increase more slowly and the increase in urate is at least in part dependent on brain activity. Perfusate samples produce chemiluminescence (Figure 16) of which the greatest contribution is due to hydrogen peroxide and is thereby abolished when samples are pretreated with catalase (see Figure 17). The amount of hydrogen peroxide-induced chemiluminescence decreases dramatically during cyanide exposure. In fact, there is a tightly coupled inverse relationship between the amount of hydrogen peroxide formed and the antioxidant (e.g. ascorbate and urate) levels in the perfusates. It is known that cyanide can induce lipid peroxidation (Johnson *et al.*, 1987). The lipid cell membranes bathed by the extracellular fluid are potentially highly vulnerable to oxidative damage during cyanide exposure because energy production is reduced and oxygen tension remains high. Fortunately, two important events occur during cyanide exposure that limit cellular damage;

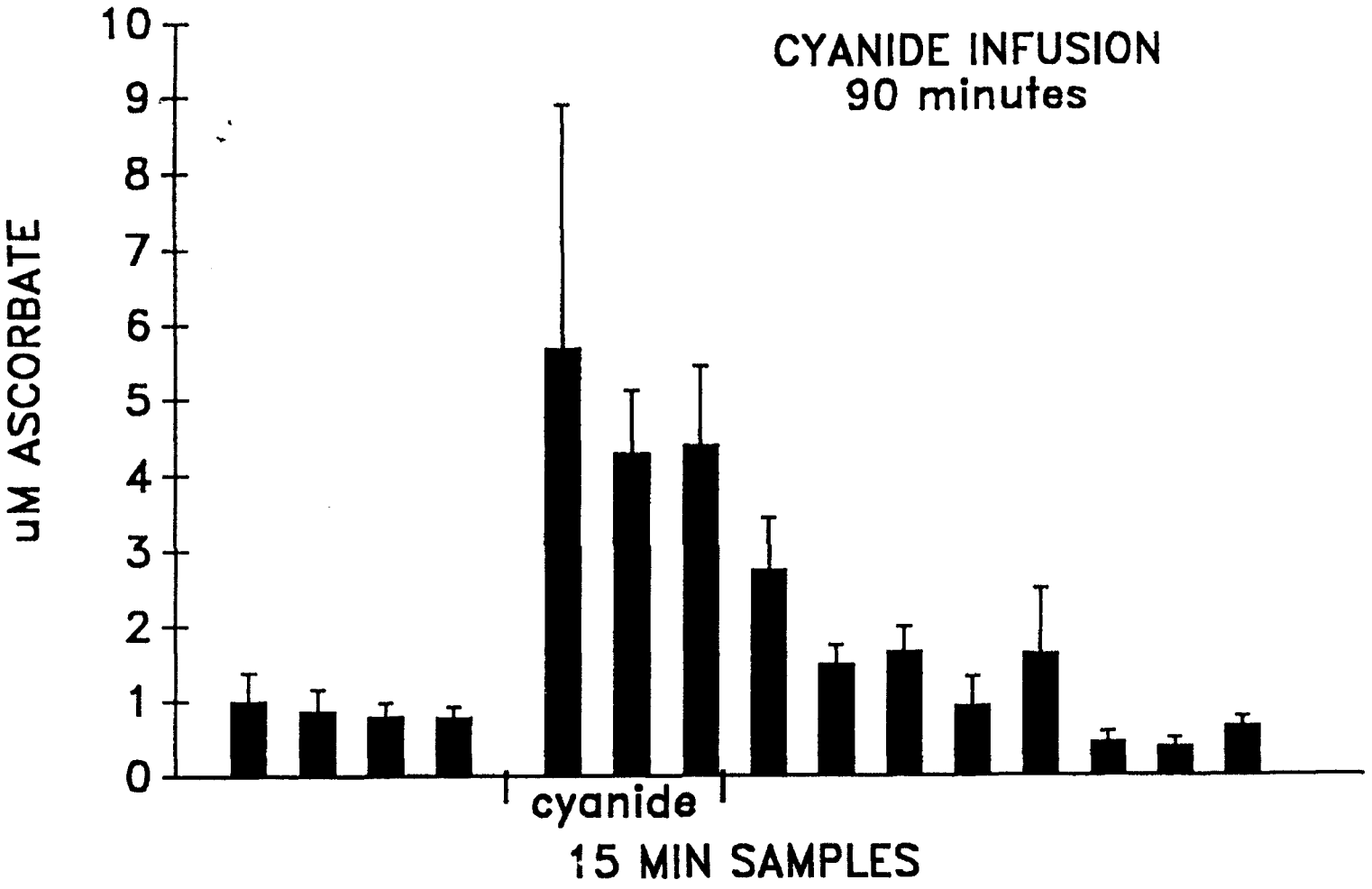

Figure 14. Concentration of ascorbate (μM) in microdialysis perfusates before, during and after cyanide exposure. A microdialysis fiber was implanted into the right piriform cortex and NaCN was given by intraveneous infusion as stated in methods for 90 minute at times indicated on the graph. The 15 minute alternate samples were analyzed. N = 8.

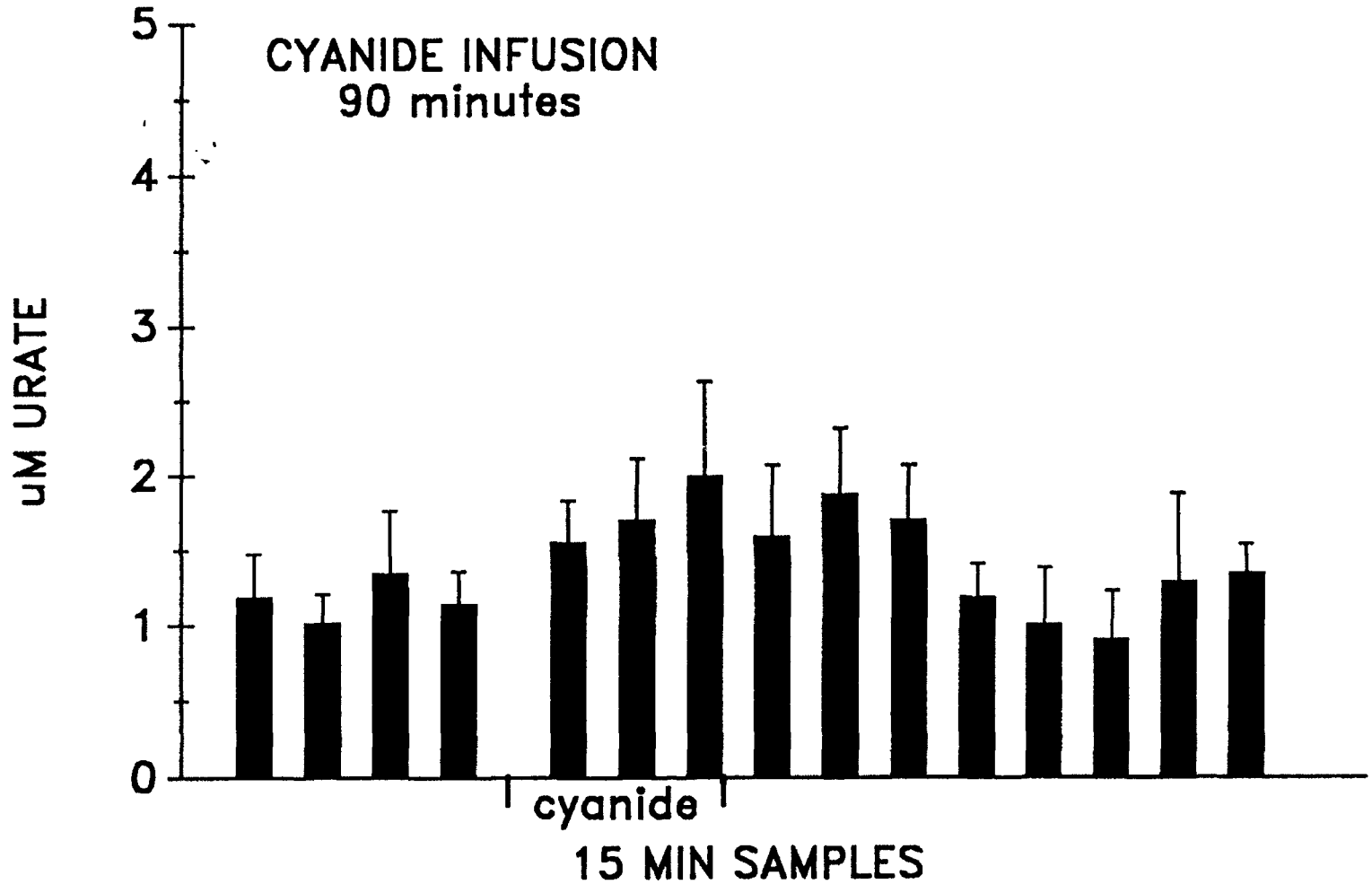

Figure 15. Concentration of urate (μM) in microdialysis perfusates before, during and after cyanide exposure. A microdialysis fiber was implanted into the right piriform cortex and NaCN was given by intraveneous infusion as stated in methods for 90 minute at times indicated on the graph. The 15 minute alternate samples were analyzed. N = 8.

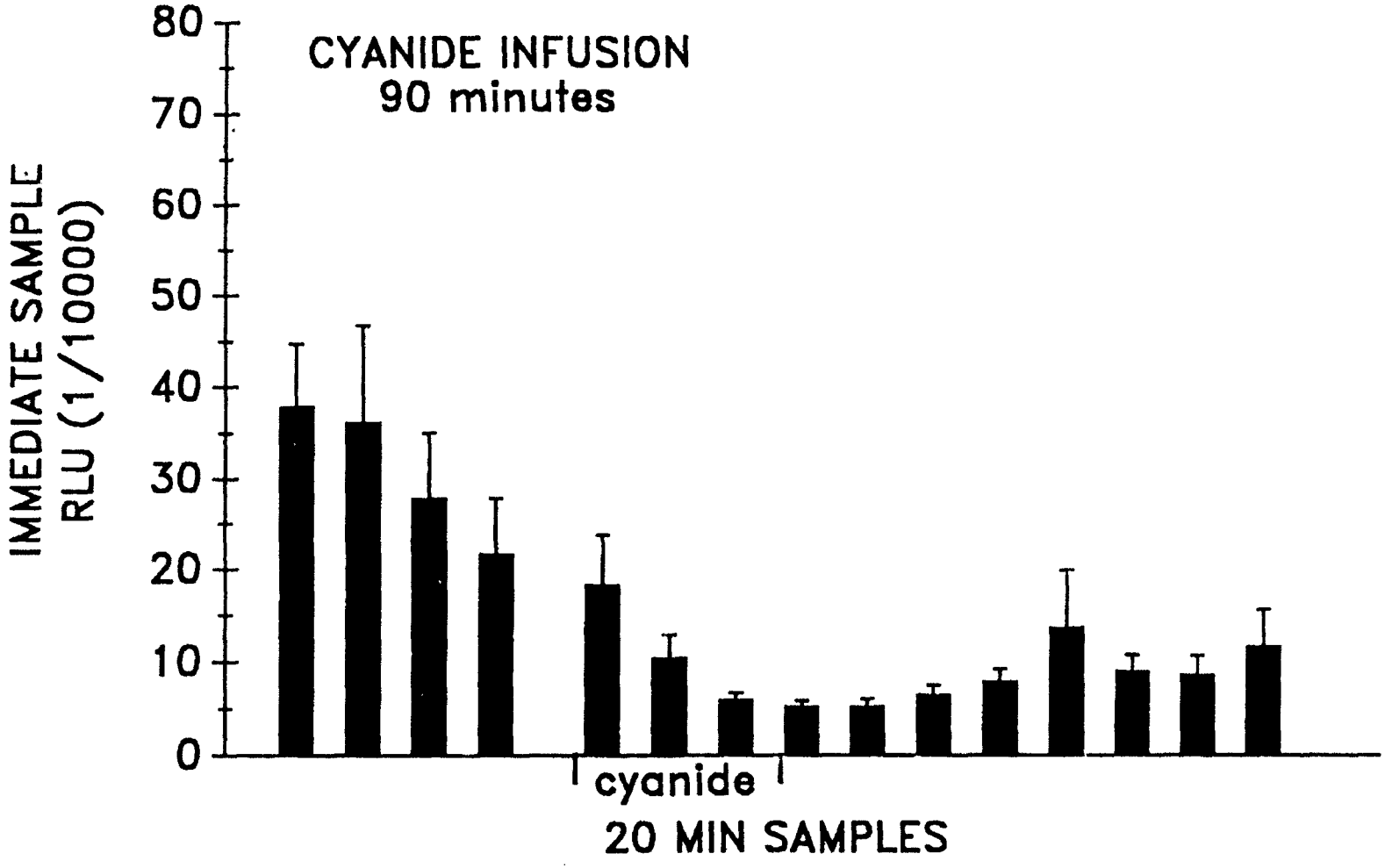

Figure 16. Chemiluminescence (RLU; relative light units) of microdialysis perfusates before, during and after NaCN exposure. A microdialysis fiber was implanted into the right piriform cortex and NaCN was given by intraveneous infusion as stated in methods for 90 minute at times indicated on the graph. The 20 minute alternate samples were analyzed. N = 8.

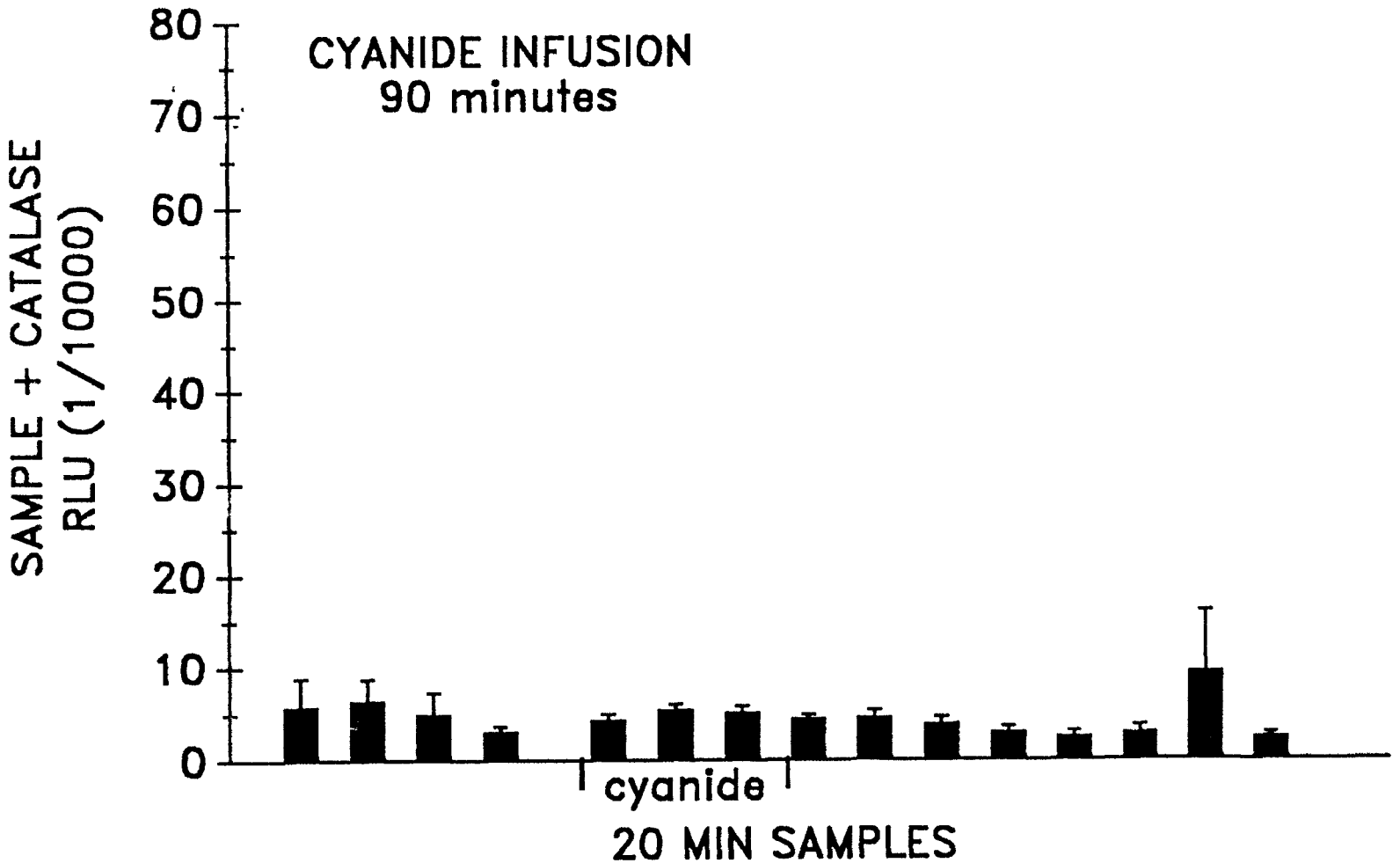

Figure 17. Catalase-resistant chemiluminescence (RLU; relative light units) of microdialysis perfusates before, during and after NaCN exposure. A microdilaysis fiber was implanted into the right piriform cortex and NaCN was given by intraveneous infusion as stated in methods for 90 minute at times indicated on the graph. The 20 minute alternate samples were analyzed. N = 8.

that is a decrease in brain activity and an increase in antioxidants in the ECF. Both events help keep reactive oxidant species low (see Figure 16) in the extracellular domain.

We propose that brain insults from a variety of causes, such as hypoxia/ischemia, brain trauma, seizures or neurotoxic chemical warfare agents (e.g. soman, cyanide) lead to the release of excitatory amino acids (EAA's) such as glutamate. The EAA's act on various subpopulations of glutamatergic receptors to produce osmotic swelling and calcium overload (Pazdernik *et al.*, 1992). This leads to a cascade of events that converge towards the formation of oxygen free radicals and nitric oxide as well as the possibility of overwhelming the antioxidant defenses. There is growing evidence that nitric oxide is synthesized in postsynaptic neurons stimulated by glutamate. It then diffuses to surrounding cells where it can mediate many functions via activation of cytoplasmic guanylyl cyclase. This can occur in neuronal, glial and vasculature cells. Moreover, there is even greater evidence that a calcium overload can lead to the formation of oxygen free radicals. Further, it is believed that oxygen free radicals can escape intracellular protective mechanisms and enter into the extracellular environment whereby they cause damage by lipid peroxidation. A microdialysis fiber was implanted into the right piriform cortex to determine if glutamate or other amino acids change in the ECF after cyanide exposure. The results shown in Figures 18-20 indicate that glutamate (Figure 18), taurine (Figure 19) but not glutamine (Figure 20) change after cyanide exposure. Aspartate levels were variable and there were no significant changes in serine, glycine or asparagine. Perfusates were collected for 2.5 hours after cyanide exposure was stopped and then the 2-DG procedure was performed to determine if brain damage had occurred. Representative 2-DG autoradiograms are illustrated in Figure 21. Damage was evident in 4 brains whereas no damage was detected in 4 other brains after cyanide exposure. Upon further evaluation of amino acid changes, it was noted that amino acid changes only occurred where there was evidence of brain damage

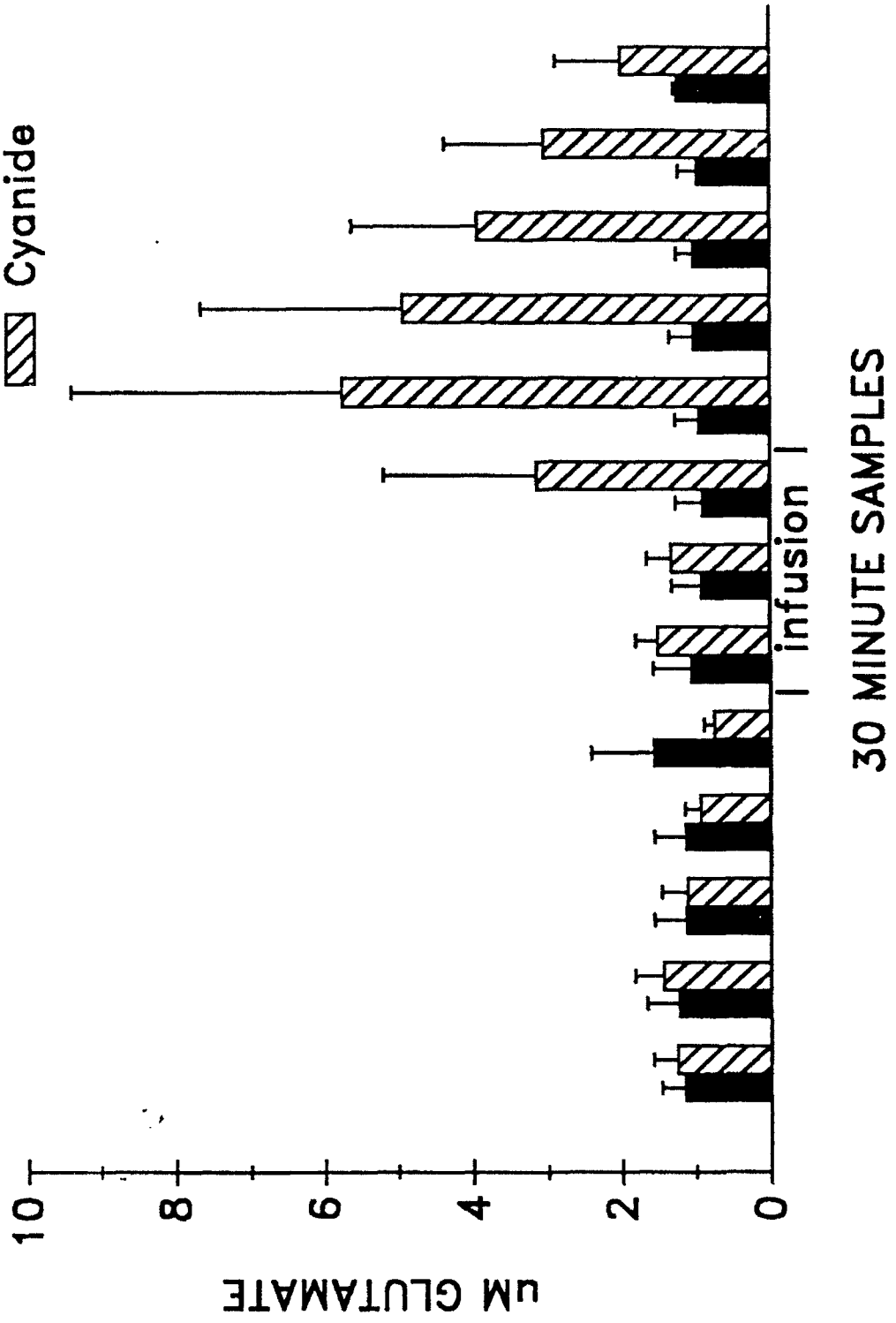

Figure 18. Concentration of glutamate (μM) in microdialysis perfusates before, during and after cyanide exposure. A microdialysis fiber was implanted into the right piriform cortex. Rats were given intraveneous saline or NaCN as stated in methods. NaCN was given for 90 minutes at times indicated on the graph. N= 2, saline group; N = 8, cyanide group.

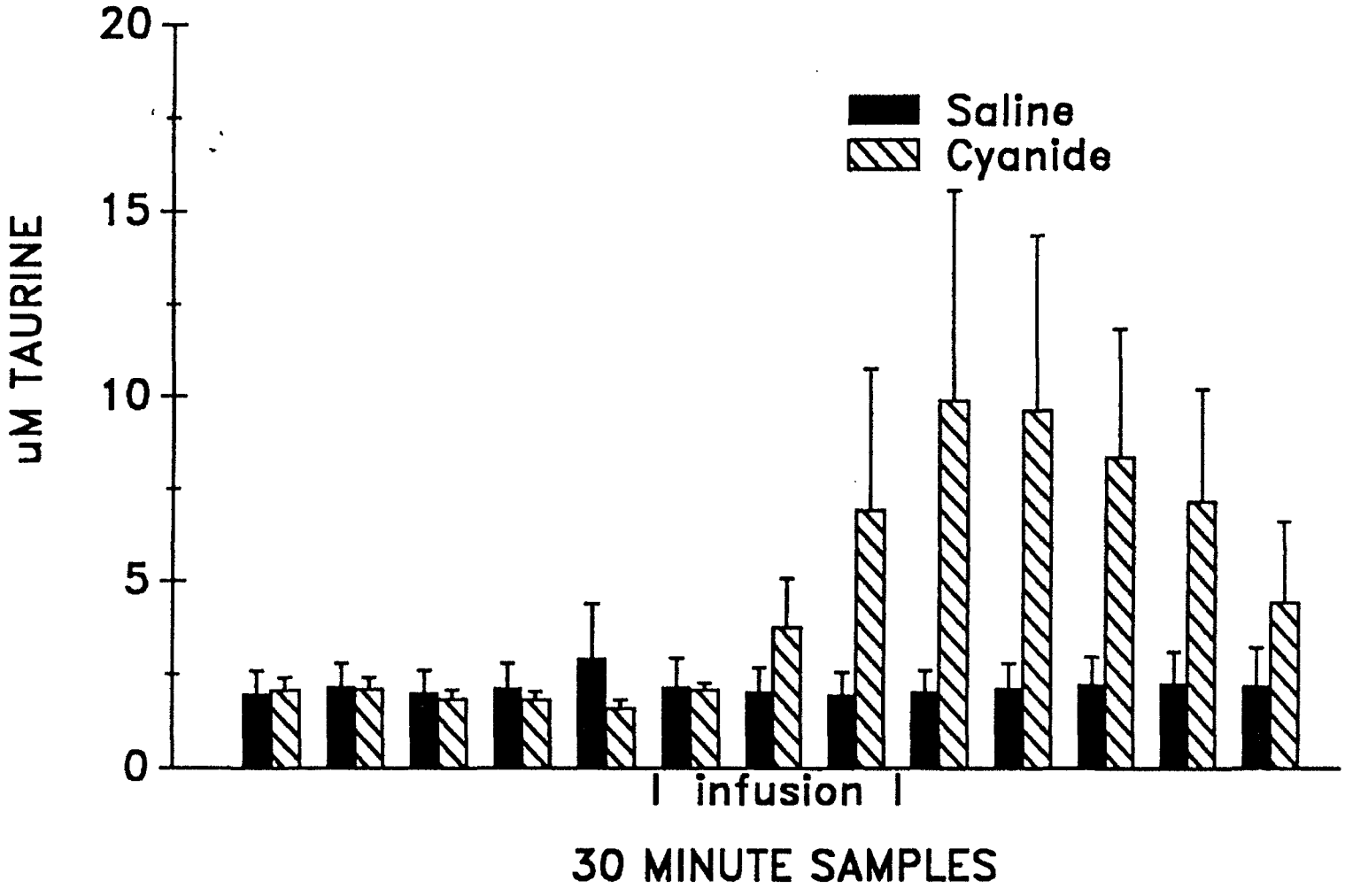

Figure 19. Concentration of taurine (μM) in microdialysis perfusates before, during and after cyanide exposure. A microdialysis fiber was implanted into the right piriform cortex. Rats were given intraveneous saline or NaCN as stated in methods. NaCN was given for 90 minutes at times indicated on the graph. N= 2, saline group; N = 8, cyanide group.

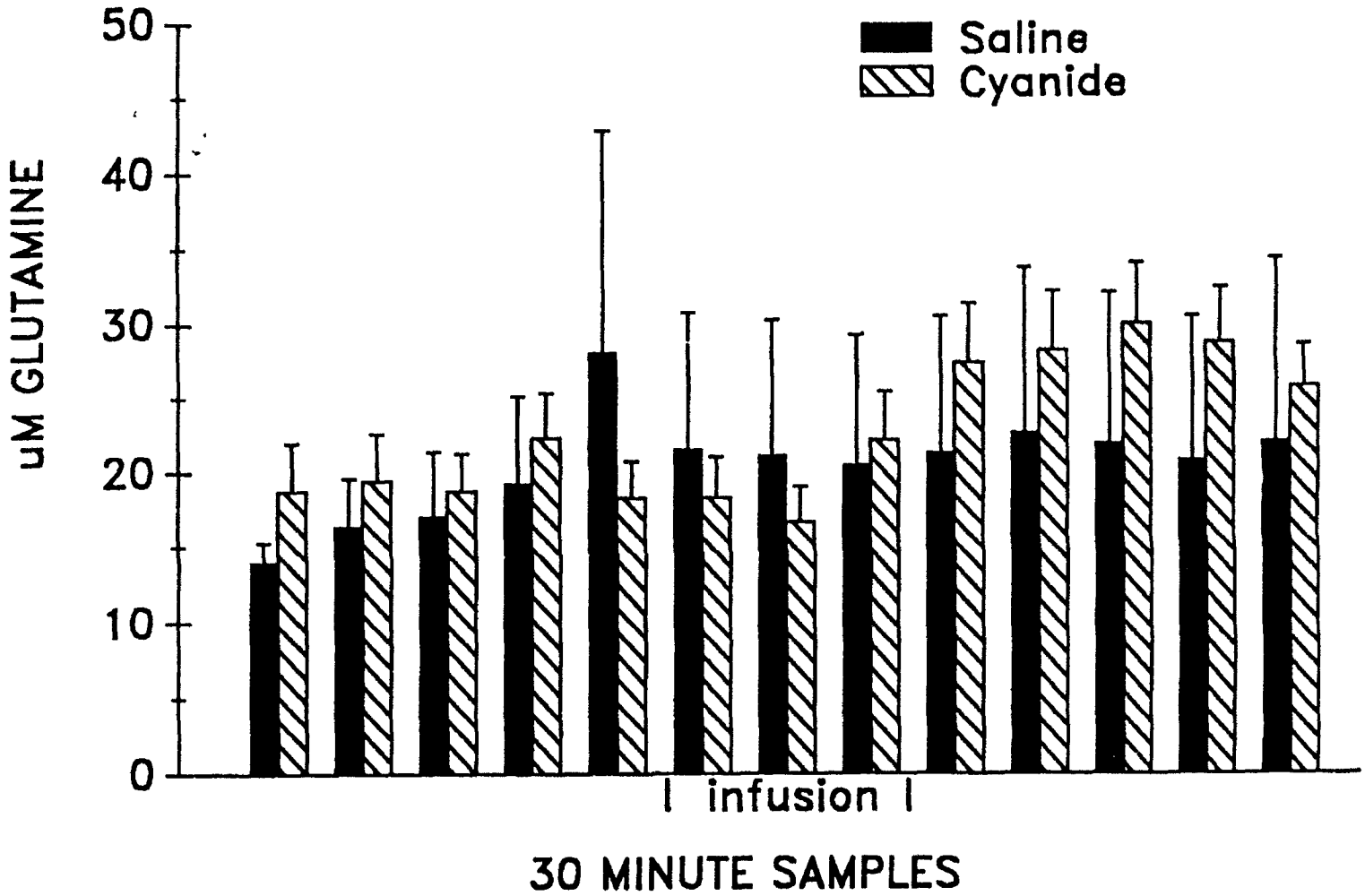

Figure 20. Concentration of glutamine (μM) in microdialysis perfusates before, during and after cyanide exposure. A microdialysis fiber was implanted into the right piriform cortex. Rats were given intraveneous saline or NaCN as stated in methods. NaCN was given for 90 minutes at times indicated on the graph. N= 2, saline group; N = 8, cyanide group.

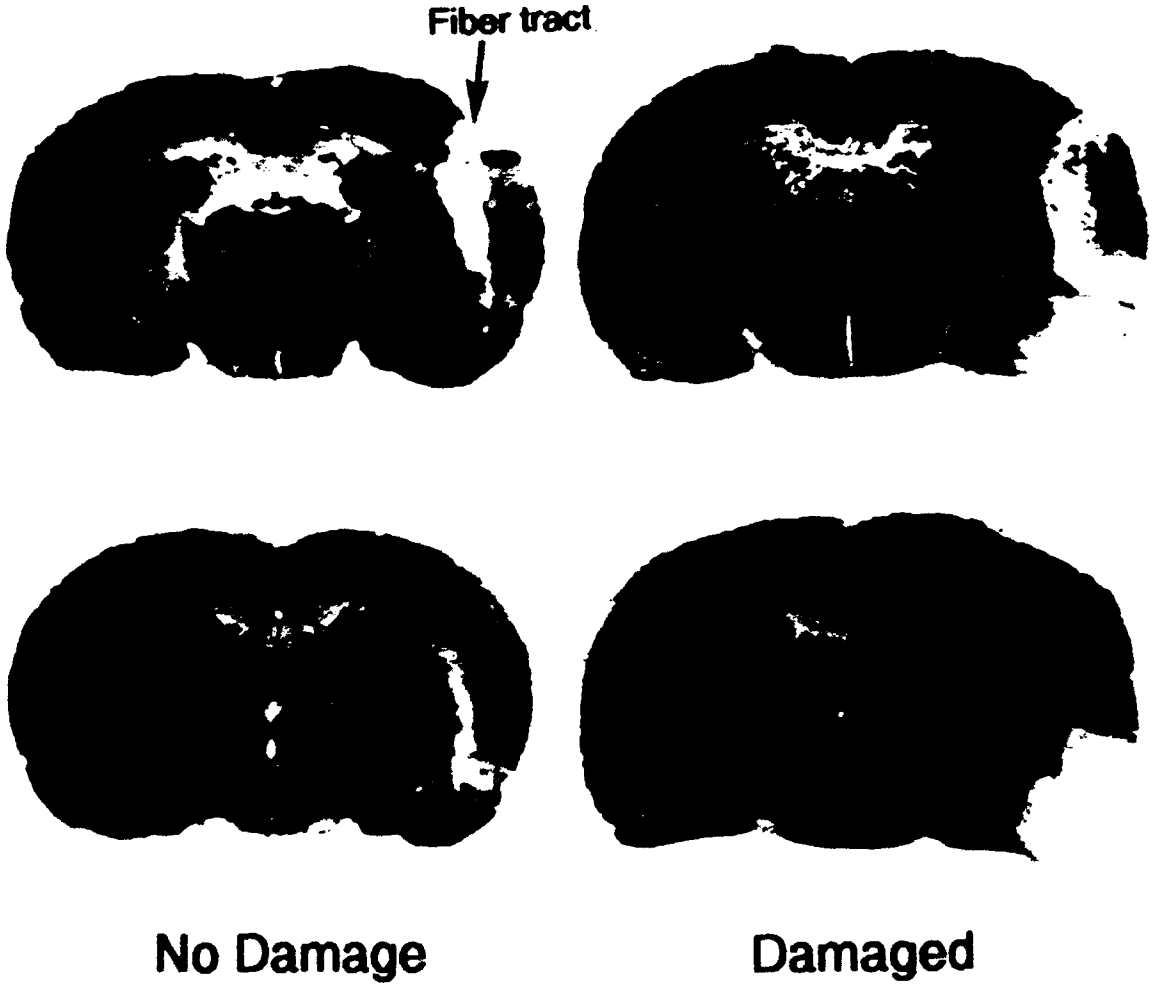

Figure 21. Representative 2-deoxyglucose autoradiograms showing LCGU in brains with and without notable brain damage.

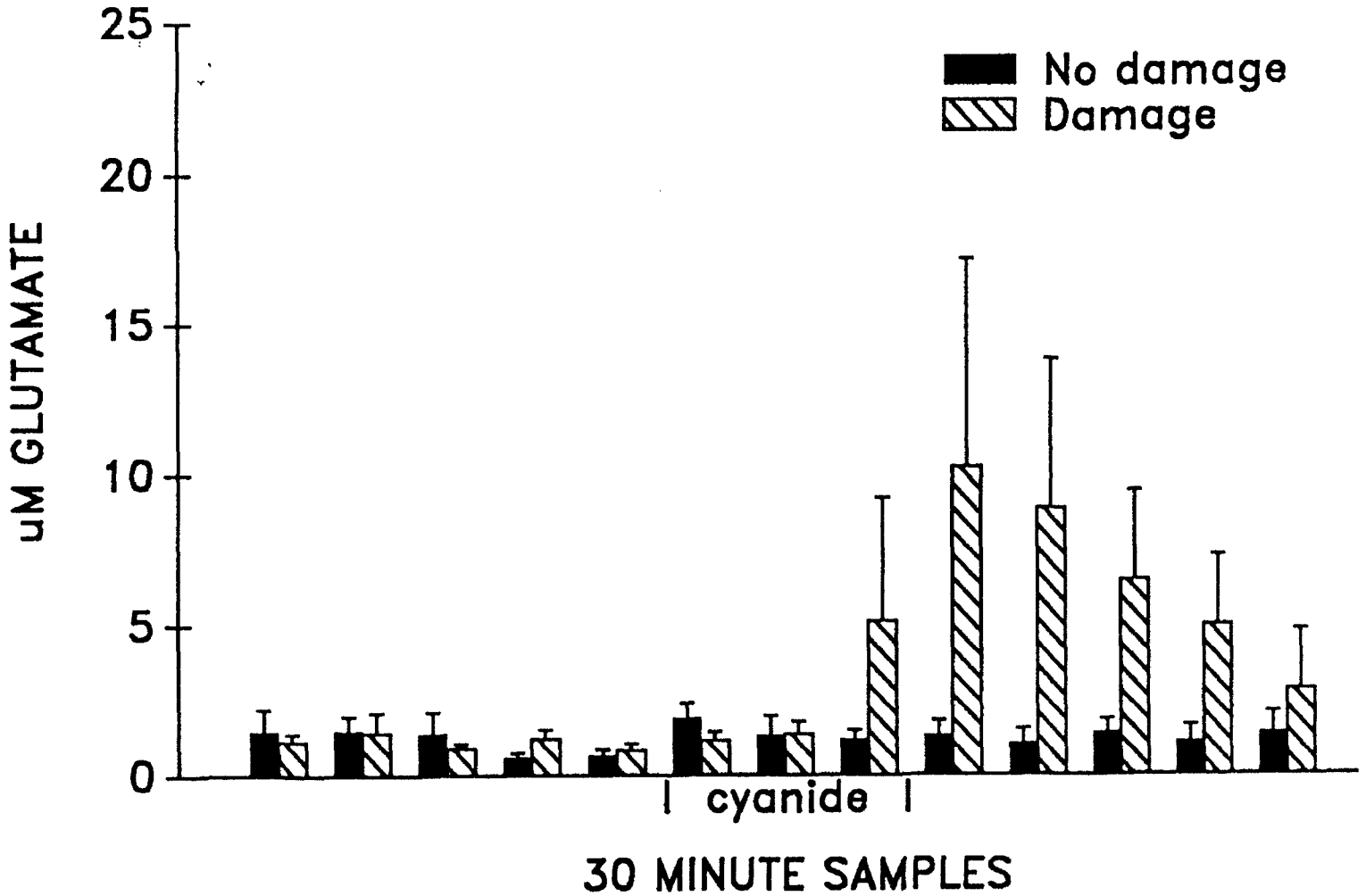

Figure 22. Concentration of glutamate (μM) when the results from Figure 18 were divided according to the evidence of brain damage. N = 4, no damage; N = 4, damage.

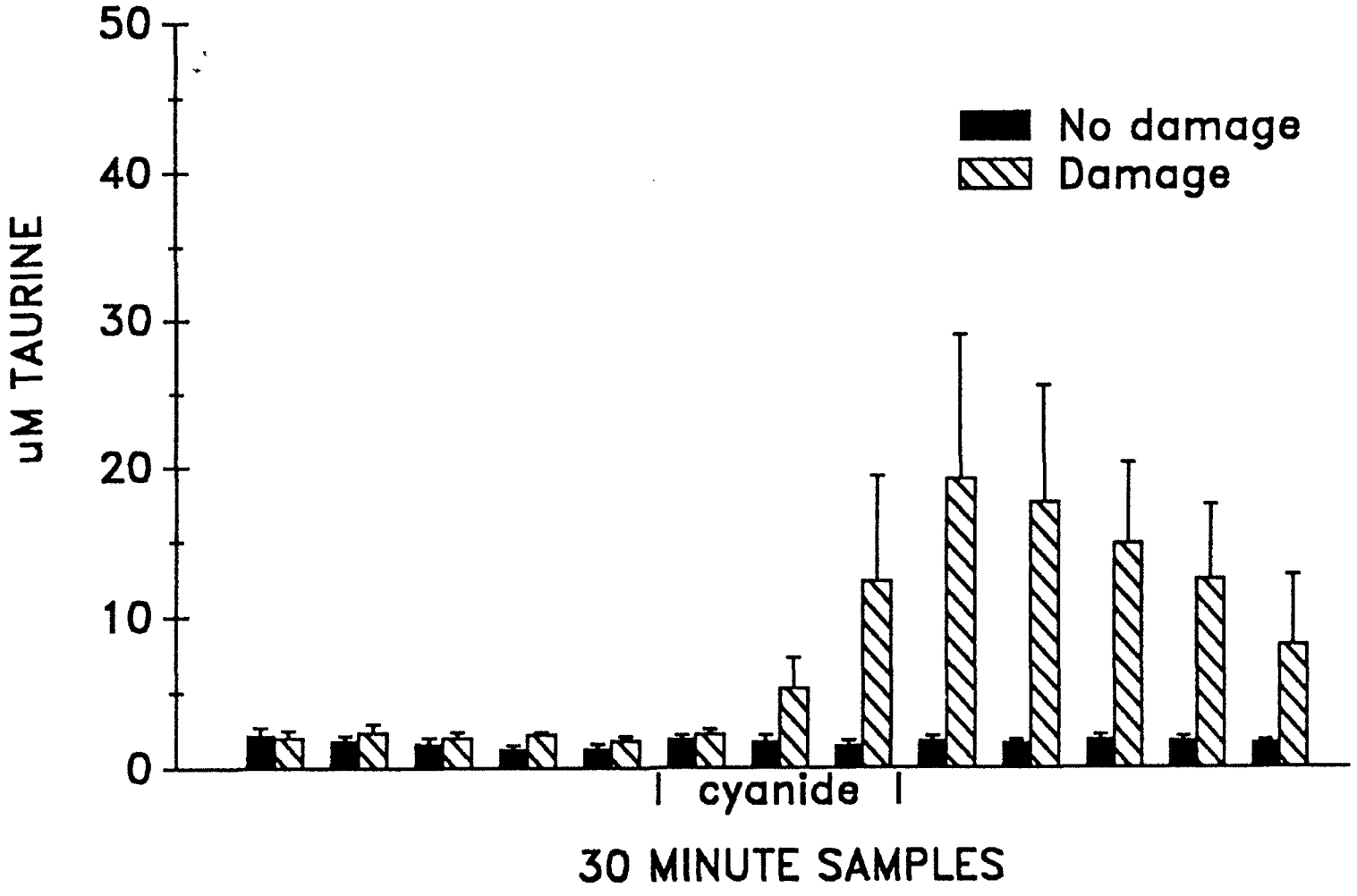

Figure 23. Concentration of taurine (μM) when the results from Figure 19 were divided according to the evidence of brain damage. N = 4, no damage; N = 4, damage.

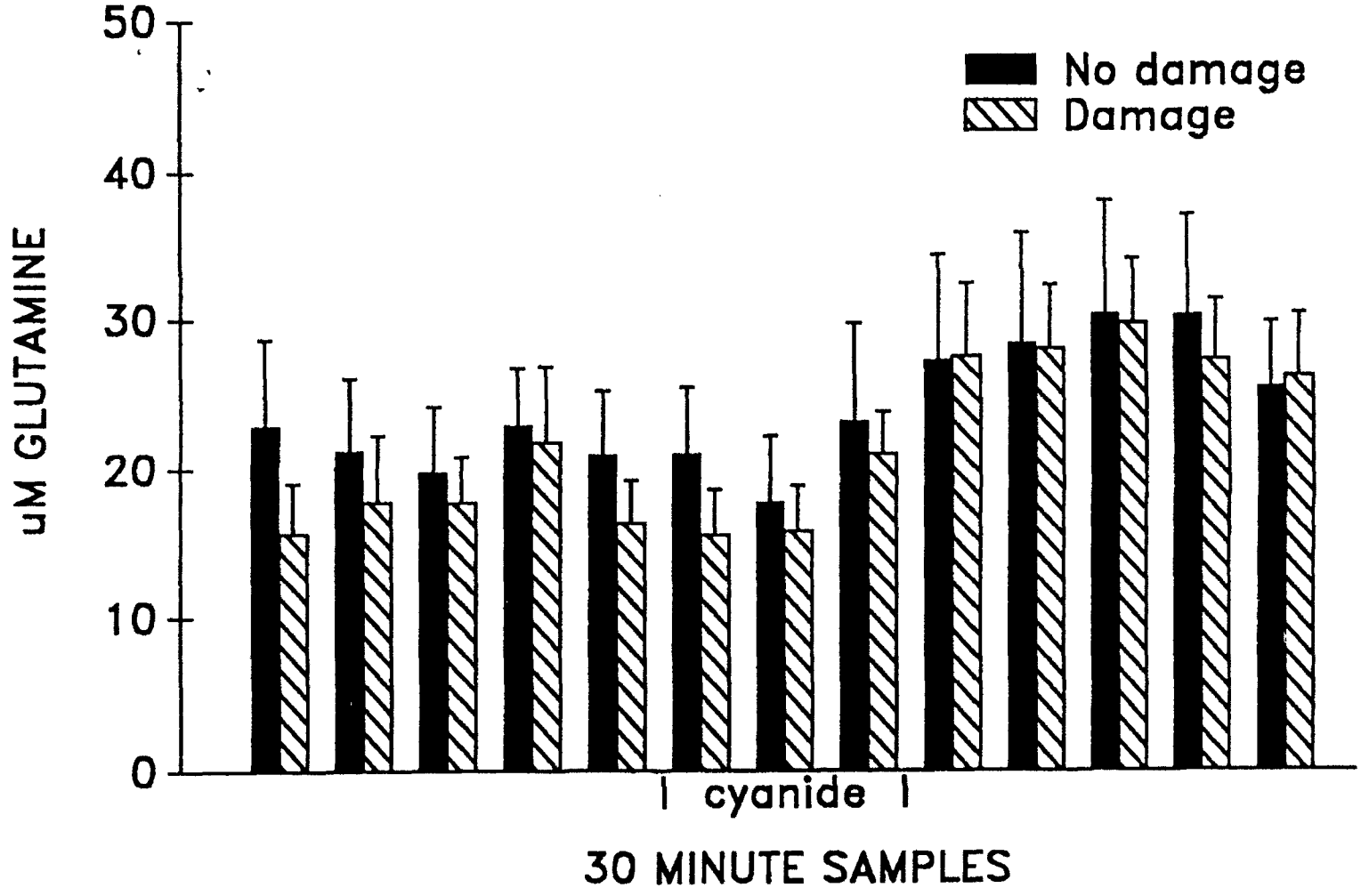

Figure 24. Concentration of glutamine (μM) when the results from Figure 20 were divided according to the evidence of brain damage. N = 4, no damage; N = 4, damage.

(see Figures 22-24). These results indicate that even with the decrease in brain activity and the increase in extracellular antioxidants after cyanide exposure brain damage still can occur in some animals. The damage that ensues may be mediated by an increase in excitatory amino acids (see Figures 22-24). These results also confirm earlier results from our laboratory (Wade *et al.*, 1987, 1988) that an increase in extracellular taurine is an excellent biochemical marker of events that lead to cellular swelling.

Brain edema studies: To determine if cyanide exposure affects energy utilization and thereby causes cellular swelling, tissue specific gravity was determined to assess brain edema as outlined below. Rats were infused with either saline or NaCN (20 μl/min; 4.5 mg/ml) into the femoral vein. The infusion was temporarily halted when the rat lost its righting reflex, and infusion was resumed when the righting reflex recurred. In the first experiment (Figure 25), rats were exposed to saline (N = 9) or NaCN (7.98 ± 1.33 mg/kg; N = 8) for 1 hour and the specific gravity of brain regions was assessed 2 hours after the initiation of the infusion. Specific gravity was slightly reduced in all brain areas and was markedly reduced in caudate and corpus callosum. Thus, these data show that there is extensive edema in the caudate and corpus callosum. The edema in corpus callosum, a primarily white matter structure, is unexpected if the major toxicity of cyanide exposure is presumed to be an interference with energy (ATP) production since the rate of energy use in white matter normally is much lower than in gray matter. The "balance" between energy reserves and rates of utilization may be involved, or possibly there is a difference in the neurochemical composition of the corpus callosum.

In the second experiment (Figure 26), rats were infused with saline (N = 6), NaCN (1 hour; 5.45 ± 0.79 mg/kg; N = 6) or NaCN (2 hours; 14.27 ± 3.08 mg/kg; N = 6) and specific gravity was determined 24 hours after initiation of infusion. At this time, there was no significant edema in any

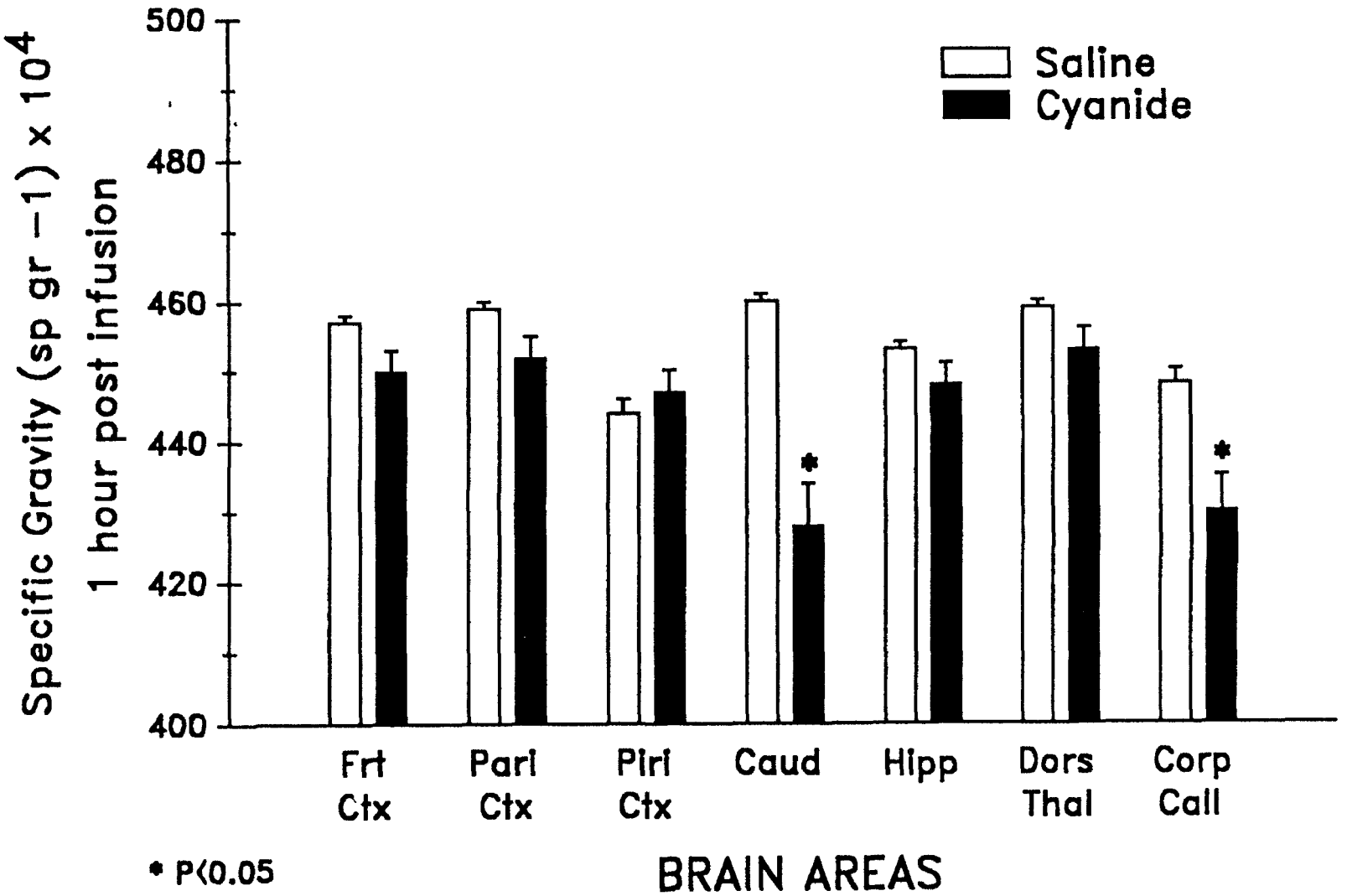

Figure 25. Specific gravity of given brain areas two hours after the initiation of a 1 hour infusion of cyanide. Rats were infused with either saline (N = 9) or NaCN (20 µl/min; 4.5 mg/ml) (N = 8) in the femoral vein for 1 hour as described in the text. Specific gravity was measured on different brain regions 2 hours after the initiation of NaCN infusion. * indicates that the cyanide-exposed group is significantly different from saline-exposed group (Student's t-test, $p < 0.05$).

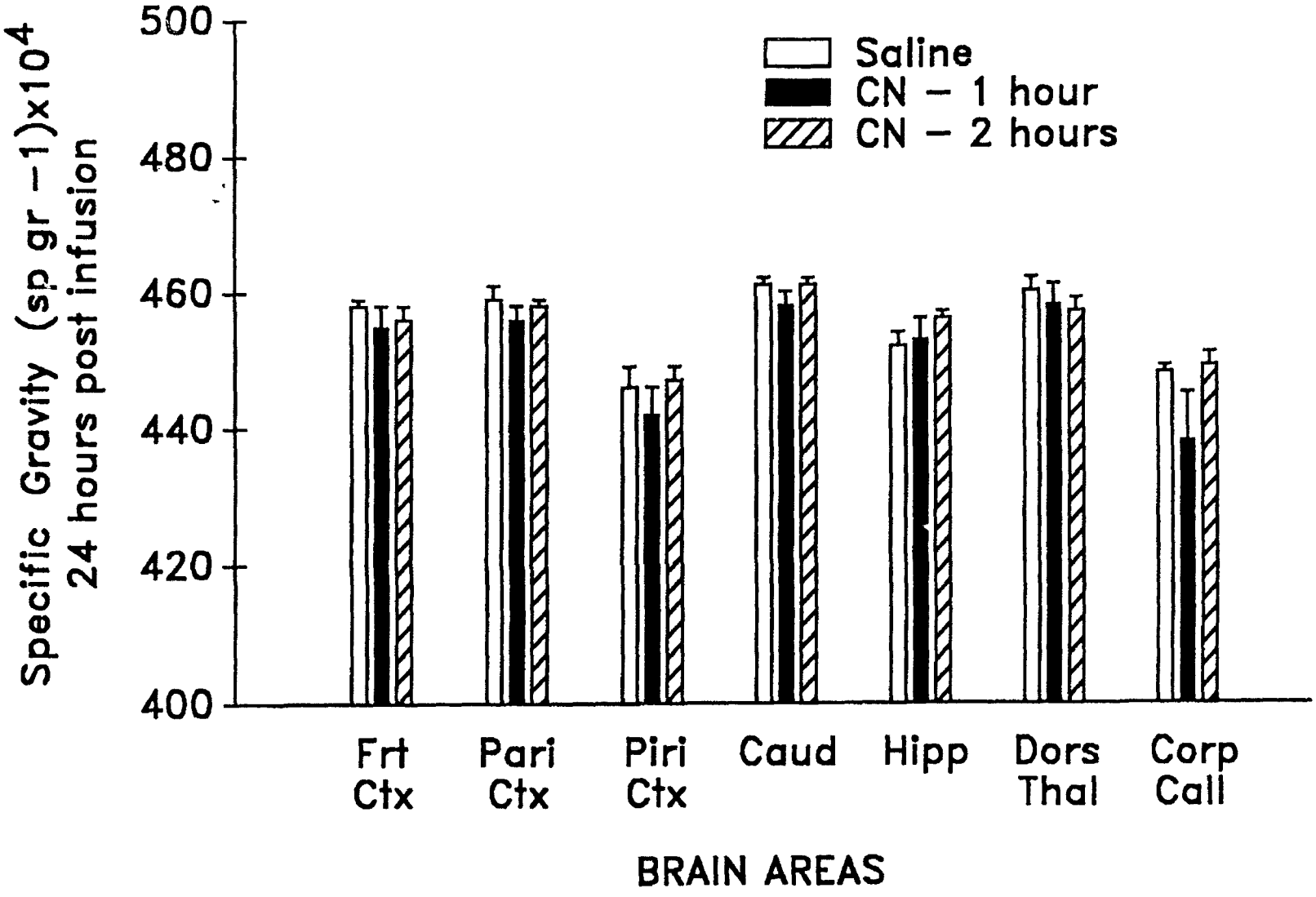

Figure 26. Specific gravity of given brain areas 24 hours after the initiation of a 1 or 2 hour infusion of cyanide. Rats were infused with saline (N = 6), NaCN (1 hour; N = 6) or NaCN (2 hours; N = 6) as described in Figure 25. Specific gravity was determined 24 hours after the initiation of NaCN infusion. The cyanide-exposed groups were not significantly different than the control group at the 0.05 level (Student's t-test).

of the brain regions, indicating that early edema is reversible. This is in agreement with the minimal neuropathology observed in similar exposed rats.

In the third experiment rats were exposed to saline (N = 3) or NaCN (N = 15) for 2 hours per day for 4 consecutive days. Eight rats died of NaCN exposure on day 1, 1 died on day 3 and 3 died on day 4. An interesting finding was that the rats required a larger dose of cyanide on each consecutive day to lose their righting reflex. The time to loss of righting reflex for the survivors is plotted in Figure 27. On day 1, it took 6.14 ± 0.64 minutes of NaCN infusion (20 µl/min; 4.5 mg/ml); on day 2, 14.36 ± 3.50 minutes, on day 3, 27.62 ± 3.58 minutes and on day 4, 29.67 ± 6.20 minutes for the rats to lose their righting reflex. The 7 rats that survived the first day of cyanide exposure on subsequent days required a large dose of cyanide to cause the first loss of righting reflex. Thus, they appeared to develop a tolerance to the loss of righting reflex. It is not clear whether or not rats that survived the first day of exposure were more resistant to cyanide lethality. The experiments were not designed to determine if tolerance occurs to cyanide lethality upon daily exposure. The specific gravity of brain tissues was assessed 24 hours after the last exposure and compared to tissues taken from three control rats that had been infused with saline (see Figure 28). Two out of the three rats had a decrease in specific gravity in the caudate and corpus callosum. Thus, these two structures appear to be the most vulnerable to NaCN induced perturbations.

Neuropathology studies: Histological studies were done on tissue from 3 rats exposed to cyanide for 2 hours. Control rats were infused for 2 hours with normal saline. Twenty-four hours later these rats were anesthetized with pentobarbital and the left ventricle cannulated after the thoracic cavity was opened. The brain was fixed by first clearing the vasculature with 20 ml of saline. This was followed with a mixture of paraformaldehyde (2%) and glutaraldehyde (2.5%) in 0.1 M phosphate buffer. The brain was next removed and immersion fixed in the same fixative for

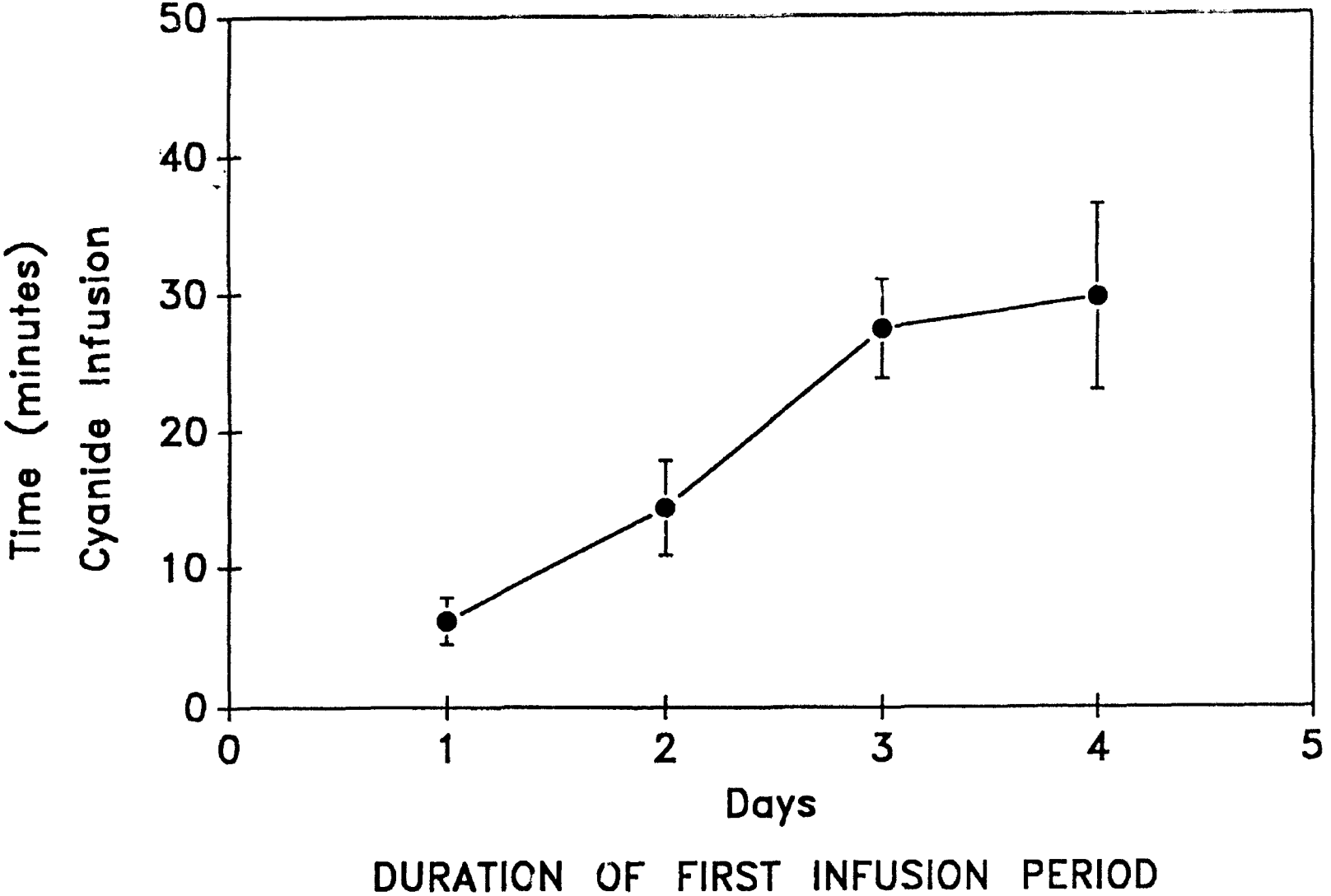

Figure 27. Duration of cyanide infusion period (minutes) on consecutive days to cause the first loss of righting reflex. Rats were infused with saline (N = 3) or NaCN (N = 15) as described in Figure 7 for 2 hours/day for 4 consecutive days. Time (minutes) of cyanide infusion to cause the first loss of righting reflex is plotted for each consecutive day.

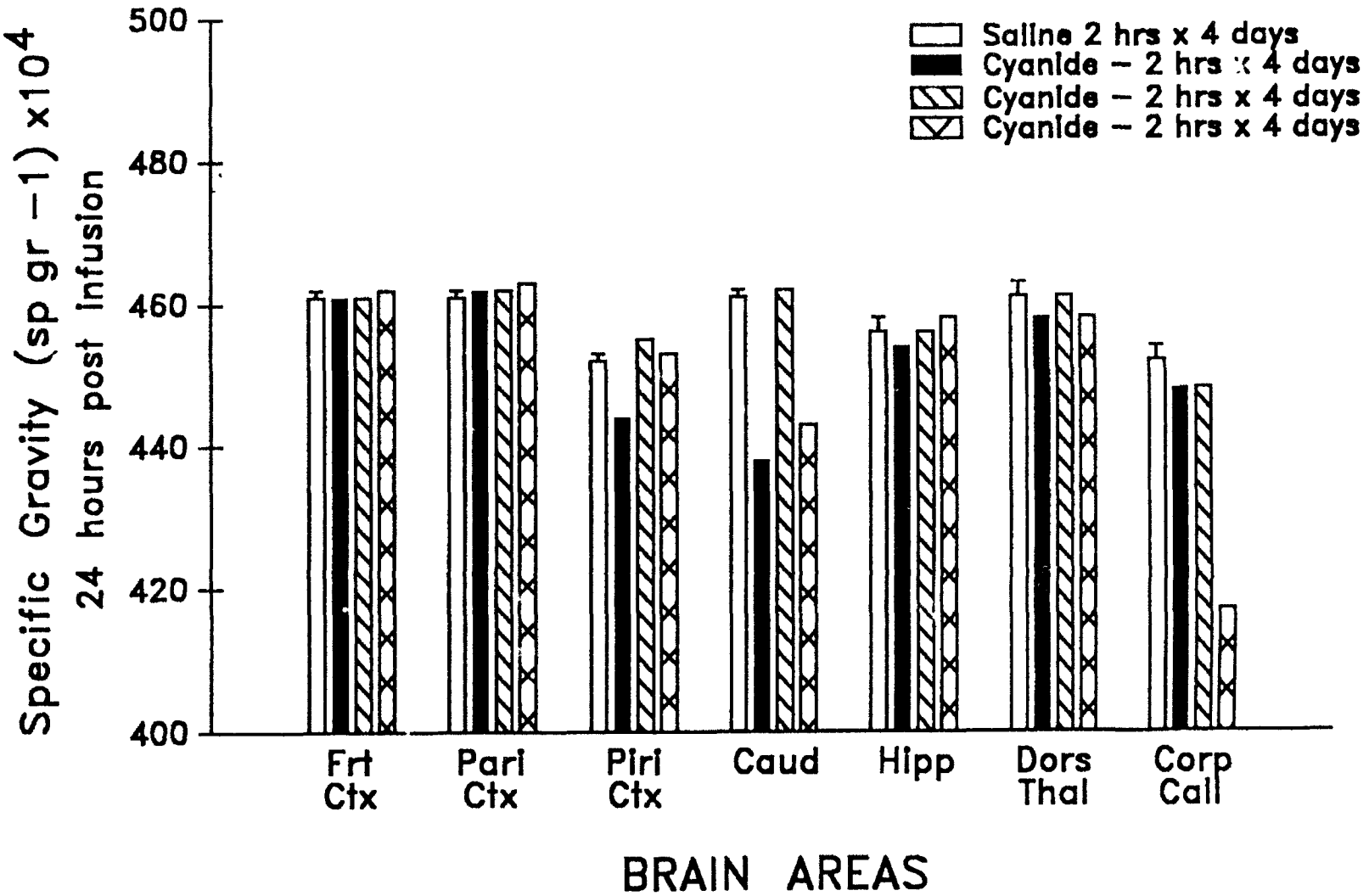

Figure 28. Specific gravity in given brain areas 24 hours after the last of 4 daily 2 hour infusion periods of cyanide. Specific gravity was determined 24 hours after the last exposure for animals that survived the infusion regimen described in Figure 27. There was a marked decrease in specific gravity in the caudate of 2 rats and in the corpus callosum in 1 rat. Saline, N = 3.

3-5 days. The brain was then paraffin mounted and a central tissue block sectioned at 5 μm and stained with H&E.

Examination of the tissue sections showed that the tissue structures were well maintained, at least as assessed by H&E histology. The pyramidal cell layer of the hippocampus appeared to have a few clumps of dark staining, contracted neurons, but the same changes were seen in the control rats. The white matter was compact with no evidence of demyelination or edema.

Our observation with H&E stained sections did not reveal significant tissue damage 24 hours after a 2-hour intermittent cyanide exposure.

CONCLUSIONS

These studies support our original hypothesis that sublethal doses of cyanide cause a shift from aerobic to anaerobic metabolism. However, an even more important aspect of these studies is the marked decrease in brain metabolism after 1 hour of cyanide exposure. This marked reduction of brain activity after acute exposure of cyanide could be a double-edged sword. On the one hand, this depression of brain activity is most likely responsible for death (i.e., inhibition of central control of vital functions) whereas, on the other hand, this cyanide-induced depression of brain activity could contribute to the minimal neuropathology observed in our study as well as in others (e.g. MacMillan, 1987; Brierley, 1976, 1977) after acute cyanide exposure. This marked depression of metabolic activity that we have observed correlates well with the cyanide-induced silent EEG described by others (MacMillan, 1987; Brierley, 1976, 1977) and the suppression of neural and synaptic function produced in hippocampal slices exposed to cyanide (Aitken and Braitmen, 1989). Still, the most important unresolved question regarding cyanide exposure is to understand the chemical and/or neural basis for cyanide-induced brain depression. Our microdialysis studies provided some important insights. The studies on lactate and pyruvate definitely confirmed our interpretation of the 2-DG studies that there was a shift from aerobic to anaerobic metabolism. The dramatic increase in monoamine acid metabolites (HVA, DOPAC and HIAA) are indicative of a marked increase in the release of dopamine and serotonin. These findings suggest similarities between cyanide-induced coma and brain ischemia. Moreover, these substances are likely candidates for triggering the suppression of brain activity. However, if these monoamines are responsible for decreasing brain activity they must trigger a neuronal response that is spread throughout the brain since depression of brain activity was found at sites very remote to local cyanide delivery to the striatum via microdialysis. Further, our studies on redox active substances in the ECF point to the importance of redox mechanisms in maintaining normal cellular function; when the antioxidant protective

mechanisms are overwhelmed dysfunction or damage ensues. The mechanisms by which extracellular ascorbate levels rapidly increase after cyanide exposure needs further investigation. Grünewald (1993) published an excellent review on factors that contribute to an increase in ECF ascorbate. These include: 1) the co-release of ascorbate and catecholamines, 2) depolarization-mediated release of ascorbate, 3) the counter exchange of ascorbate and glutamate, and 4) glutamate-induced release of ascorbate via activation of the NMDA receptor. These factors may all contribute in part to the rapid increase in ECF ascorbate after cyanide exposure. The rapid increase in extracellular ascorbate definitely protects the extracellular domain from excessive oxidative damage after cyanide exposure. However, there is good reason to believe that in cyanide-induced neurotoxicity, lipid peroxidation occurs (Johnson *et al.,* 1987). Moreover, when damage occurs, we have good evidence that EAA are involved. The studies presented demonstrate that understanding the changes in extracellular chemistry, sampled by microdialysis, provides a wealth of information on how toxic chemicals affect the brain. There needs to be considerably more effort towards understanding the complex relationships between redox-active substances, monoamines and EAA in normal brain function and brain dysfunction produced by chemical warfare agents. We believe that nitric oxide is an important player that needs to be studied. Our recent success with intracerebral microdialysis technology in the detection of important oxidative (e.g., hydrogen peroxide) and reductive (e.g., ascorbate) substances in the ECF provides a new window for determining the effects of cyanide on free radical-induced brain damage. This is of importance in discovering what situations (e.g., oxygen therapy, drugs) may amplify or protect against cyanide-induced neurotoxicity.

REFERENCES

Aitken, P.G. and Braitman (1989). The effects of cyanide on neural and synaptic function in hippocampal slices. Neurotoxicology 10, 239-248.

Bass, N.H. (1968). Pathogenesis of myelin lesions in experimental cyanide encephalopathy. A microchemical study. Neurology 18, 167-177.

Bhardwaj, A., Brannan, T., Martinez-Tica, J. and Weinberger, J. (1990). Ischemia in the dorsal hippocampus is associated with acute extracellular release of dopamine and norepinephrine. J. Neural Trasm. 80, 195-201.

Borowitz, J.L., Kanthasamy, A.G. and Isom, G.E. (1992). Toxicodynamics of cyanide. In: Chemical Warfare Agents (Ed. S.M. Soman), Academic Press, Inc., New York, pp. 209-236.

Brannan, T., Weinberger, J., Knott, P., Taff, I., Kaufmann, H., Togasaki, D., Nieves-Rosa, J. and Maker, H. (1987). Direct evidence of acute, massive striatal dopamine release in gerbils with unilateral strokes. Stroke 18, 108-110.

Brierley, J.B., Brown, A.W. and Calverley, J. (1976). Cyanide intoxication in the rat: physiological and neuropathological aspects. J. Neurol. Neurosurg. Psychiatry 39:, 129-140.

Brierley, J.B., Prior, P.F., Calverley, J. and Brown, A.W. (1977). Cyanide intoxication in Macaca mulatta. J. Neurol. Sci. 31, 131-157.

Burrows, G.E., Liu, D.H.W., Isom, G.E. and Way, J.L. (1982). Effect of antagonists on the physiologic disposition of sodium cyanide. J. Toxicol. Environ. Health 10, 181-189.

Funata, N., Song, S.Y., Funata, M. and Higashino, F. (1984). A Study of Experimental Cyanide Encephalopathy in the Acute Phase-Physiological and neuropathological correlation. Acta Neuropathol. 64, 99-107.

Hicks, S.P. (1950). Brain metabolism *in vivo*. 1. The distribution of regions caused by cyanide poisoning, insulin hypoglycemia, asphyxia in nitrogen and fluororacetate poisoning in rats. Arch. Pathol. 49, 111-137.

Hirano, A., Levine, S., Zimmerman, H.M. (1967). Experimental cyanide encephalopathy: electron microscopic observations of early lesions in white matter. J. Neuropath. Exp. Neurol. 26, 200-213.

Isom, G.E. and Way, J.L. (1984). Effects of oxygen on antagonism of cyanide intoxication: cytochrome oxidase *in vitro*. Toxicol. Appl. Pharmacol. 74, 57-62.

Johnson, J.D., Meisenheimer, T.L. and Isom, G.E. (1986). Cyanide induced neurotoxicity: role of neuronal calcium. Toxicol. Appl. Pharmacol. 84, 464-469.

Johnson, J.D., Conroy, W.G., Burris, K.D. and Isom, G.E. (1987). Peroxidation of brain lipids following cyanide intoxication in mice. Toxicology 46, 21-28.

Kuhr, W.G., van den Berg, C.J. and Korf, J. (1988). In vivo indentification and quantitative evalualtion of carrier-mediated transport of lactate at the cellular level in the striatum of conscious, freely moving rats. J. Cererb. Blood Flow and Metab. 8, 848-856.

Levine, S. (1967). Experimental cyanide encephalopathy: gradients of susceptibility in the corpus callosum. J. Neuropathol. Exp. Neurol. 26, 214-222.

Grünewald, R.A. (1993). Ascorbic acid in the brain. Brain Res. Rev. 18, 123-133.

Lindroth, P. and Mopper, K. (1979). High-performance liquid chromatographic determination of subpicomole amounts of amino acids by precolumn fluorescence derivatization with *o*-phthaldialdehyde. Anal. Chem. 51, 1667-1674.

MacMillan, V.H. (1987). Cerebral energy metabolism in cyanide encephalopathy. J. Cereb. Blood Flow Metab. 9, 156-162.

Nelson, S., Mantz, M.L. and Maxwell, J. (1971). Use of specific gravity in the measurement of cerebral edema. J. Appl. Physiol. 30, 268-271.

Nelson, S.R. and Olson, J.P. (1987). Role of early edema in the development of regional seizure-related brain damage. Biochem. Res. 12, 555-558.

Paxinos, G. and Watson, C. (1982). *The Rat Brain in Stereotaxic Coordinates*. Academic Pres, New York.

Pazdernik, T., Layton, M., Nelson, S.R. and Samson, F.E. (1992). The osmotic/calcium stress theory of brain damage: Are free radicals involved? Neurochem. Res. 17, 11-21.

Persson, S.A., Cassel, G. and Sellstrom, A. (1985). Acute cyanide intoxication and central transmitter systems. Fundam. Appl. Toxicol. 5, S150-S159.

Piantadosi, C.A., Sylvia, A.L. and Jöbis, F.F. (1983). Cyanide-induced cytochrome a, a_3 oxidation-reduction responses in rat brain *in vivo* . J. Clin. Invest. 72, 1224-1233.

Robinson, P.C., Baskin, S.I., Groff, W.A. and Franz, D.R. (1984). Cyanide loss from tissue baths in the presence and absence of tissue. Toxicol. Lett. 21, 305-308.

Schubert, J. and Brill, W.A. (1968). Antagonism of experimental cyanide toxicity in relation to the *in vivo* activity of cytochrome oxidase. J. Pharmacol. Exp. Ther. 162, 352-359.

Slivka, A., Brannan, T.S., Weinberger, J., Knott, P.J. and Cohen, G. (1988). Increases in extracellular dopamine in striatum during cerebral ischemia: A study utilizing cerebral microdialysis. J. Neurochem. 50, 1714-1718.

Sokoloff, L. (1976). Mathematical analysis and determination of the "lumped constants". Neurosci. Res. Program Bull. 14, 466-468.

Sokoloff, L. (1981). The relationship between function and energy metabolism: its use in the localization of functional activity in the nervous system. Neurosci. Res. Program Bull. 19, 159-210.

Sokoloff, L., Reivich, M., Kennedy, C., Des Rosiers, M.H., Patlak, C.S., Pettigrew, K.D., Sakurada, O. and Shimohara, M. (1977). The [^{14}C]deoxyglucose method for the measurement of local cerebral glucose utilization: theory, procedure and normal values in the conscious and anesthetized albino rat. J. Neurochem. 28, 897-916.

Wade, J., Samson, F., Nelson, S. and Pazdernik, T. (1987). Changes in extracellular amino acids during soman and kainic acid-induced seizures. J. Neurochem. 49, 654-650.

Wade, J., Olson, J., Samson, F., Nelson, S. and Pazdernik, T. (1988). A possible role of taurine in osmoregulation within the brain. J. Neurochem. 51, 740-745.

Way, J.L. (1984). Cyanide intoxication and its mechanism of antagonism. Ann. Rev. Pharmacol. Toxicol. 24, 451-481.

Weinberger, J. and Nieves-Rosa, J. (1987). Metabolism of monoamine neurotransmitters in the evolution of infraction in ischemic striatum. J. Neural. Transm. 69, 265-275.

Westerink, B.H., Hofsteede, H.M., Damsma, G. and deVries, J.B. (1988). The significance of extracellular calcium for the release of dopamine, acetylcholine and amino acids in

conscious rats evaluated by brain microdialysis. Naunyn Schmiedebergs Arch. Pharmacol. 337, 373-368.

Yamamoto, Y. and Ames, B.N. (1987). Detection of lipid hydroperoxides and hydrogen peroxide at picmole levels by an HPLC and isoluminol chemiluminescence assay. Free Radical Biol. Med. 3, 359-361.

Yamazaki, Y., Imagak, M., Kiuchi, Y., Izumi, J., Matsumoto, M., Kanda, Y. and Oguchi, K. (1992). Changes in extracellular level of amino acids by NaCN perfusion in rat straitum. JPN J. Pharm. 58, Suppl. I., pp. 372.

Appendix 1. Bibliography of publication on contract DAMD17-90-C-0041

1. Layton, M., and Pazdernik, T.L. Detection of reducing substances in brain extracellular fluid via microdialysis perfusion with cytochrome C. 5th Annual M.D.-Ph.D. Conference, Aspen, Colorado, p. 6, 1990.
2. Pazdernik, T.L., S.R. Nelson, R.S. Cross and F.E. Samson. Cyanide causes unexpected changes in brain glucose use. Europ. J. Pharmacol. 183:1541-1542, 1990.
3. Savolainen, K.M., O. Muona, F.E. Samson, S.R. Nelson and T.L. Pazdernik. Lithium modifies convulsions and brain phosphoinositide turnover induced by organophosphates. Soc. Neurosci. 16:15.7, 1990.
4. Romanas, M.M., F.E. Samson, S.R. Nelson, and T.L. Pazdernik. Toxic and trophic effects of neuronal stimulation. The Frederick E. Samson Symposium on Neurochemistry, Abs. #1, 1990.
5. Layton, M.E., J.W. Shaw, S.R. Nelson, F.E. Samson, and T.L. Pazdernik. Detection of ascorbic acid release during kainic acid-induced seizures via microdialysis perfusion with cytochrome C. The Frederick E. Samson Symposium on Neurochemistry, Ab. #3, 1990.
6. Zuo, H., T.L. Pazdernik, R.S. Cross, F.E. Samson, and S.R. Nelson. Cyanide produces reversible edema prominent in caudate and corpus callosum. The Frederick E. Samson Symposium on Neurochemistry, Ab. #5, 1990.
7. Layton, M.E., T.L. Pazdernik, S.R. Nelson and F.E. Samson. Reactive oxygen species detected by microdialysis in brain extracellular fluid increase during seizures. Soc. Neuroscience 17:578.21, 1991.
8. Zuo H., S.R. Nelson, F.E. Samson, T.L. Pazdernik and J.S. Beckman. L-nitroarginine attenuates cerebral glucose use associated with kainic acid-induced seizures. FASEB J. 6:A5458, 1992.
9. Pazdernik, T.L., S.R. Nelson, R. Cross, H. Zuo and F. Samson. Cyanide actions on brain metabolism. Proceedings of the 1991 Medical Defense Bioscience Review (U.S. Army Medical Research Institute of Chemical Defense), pp 265-268.
10. Nelson, R.R., T.L. Pazdernik and F.E. Samson. Copper plus ascorbate inactivates lactate dehydrogenase: Are oxygen radicals involved? Proc. West. Pharmacol. Soc. 35:37-41, 1992.
11. Layton, M.E. and T.L. Pazdernik. Reactive oxygen species in rat brain extracellular fluid. In: Oxygen Free Radicals in Tissue Damage (Eds., C.M. Tarr and F.E. Samson), Burkhauser, Boston, MA, in press.
12. Layton, M.E., J.K. Wagner, S.R. Nelson, F.E. Samson and T.L. Pazdernik. Oxidative stress and antioxidant responses in rat piriform cortex associated with kainic acid-induced seizures. Soc. Neuroscience 18:672.12, 1992.

Several manuscripts in preparation.

Appendix 2. Personnel receiving pay from contract DAMD17-90-C-0041.

Thomas L. Pazdernik
Robert Cross
Hong Zuo
Anjana Dey

Appendix 3. Graduate degrees resulting from contract support on DAMD17-90-C-0041.

Matthew Layton (to be conferred June, 1993).